[redacted]

Copy 268
RM H54J26a

NACA RM H54J26a

NACA

CASE FILE COPY

RESEARCH MEMORANDUM

FLIGHT MEASUREMENTS OF THE DYNAMIC LONGITUDINAL STABILITY AND FREQUENCY-RESPONSE CHARACTERISTICS OF THE XF-92A DELTA-WING AIRPLANE

By Euclid C. Holleman and William C. Triplett

High-Speed Flight Station
Edwards, Calif.

CLASSIFICATION CHANGED TO UNCLASSIFIED
AUTHORITY: NASA PUBLICATION ANNOUNCEMENT NO. 2
EFFECTIVE DATE: OCTOBER 31, 1958
WHL

CLASSIFIED DOCUMENT

This material contains information affecting the National Defense of the United States within the meaning of the espionage laws, Title 18, U.S.C., Secs. 793 and 794, the transmission or revelation of which in any manner to an unauthorized person is prohibited by law.

NATIONAL ADVISORY COMMITTEE FOR AERONAUTICS

WASHINGTON

January 13, 1955

[redacted]

NATIONAL ADVISORY COMMITTEE FOR AERONAUTICS

RESEARCH MEMORANDUM

FLIGHT MEASUREMENTS OF THE DYNAMIC LONGITUDINAL STABILITY AND FREQUENCY-RESPONSE CHARACTERISTICS OF THE XF-92A DELTA-WING AIRPLANE

By Euclid C. Holleman and William C. Triplett

SUMMARY

Dynamic longitudinal maneuvers have been obtained over a Mach number range of 0.42 to 0.94 at an altitude of about 30,000 feet by utilizing the XF-92A delta-wing research airplane. An analysis of the airplane dynamic response was made using three approaches: measured period and time to damp, analogue computer simulation of the airplane time-response characteristics, and Fourier transformation. Results are presented as variations of period, time and cycles to damp, and stability derivatives with Mach number.

For the test altitude the longitudinal period and time to damp decreased with increasing Mach number. The airplane did not meet the longitudinal time-to-damp requirement of the Air Force. The airplane damping factor and control effectiveness were essentially constant and the static stability increased with Mach number.

Examination of the flight record showed little coupling, either aerodynamic or engine gyroscopic, during the longitudinal tests.

INTRODUCTION

The NACA High-Speed Flight Station has conducted a flight investigation utilizing the XF-92A airplane built by the Consolidated Vultee Aircraft Corp. Dynamic stability, handling qualities, aerodynamic loads, and lift and drag are some of the phases of this investigation that have been conducted concurrently. This paper presents the results of the investigation of dynamic longitudinal stability. Data were obtained over a Mach number range of 0.42 to 0.94 at about 30,000 feet. Results of a preliminary dynamic stability investigation were reported in reference 1. This paper presents the results of an analysis of more suitable and conclusive data than were available for reference 1. References 2 and 3 give results of other phases of testing on the airplane.

With the aid of the Ames and Langley Laboratories the analysis of the data has been completed by three methods. Analysis of the pertinent quantities from the film record was made at the High-Speed Flight Station; an analysis of the flight records was carried out on a Reeves Electric Analogue Computer by the Flight Research Branch of the Ames Laboratory; and the Fourier analysis computations were made by the data reduction section of Instrument Research Division of the Langley Laboratory. Results of these analyses are presented as stability derivatives, transfer coefficients, and frequency-response plots.

SYMBOLS

C_L	lift coefficient
C_m	pitching-moment coefficient about center of gravity
C_N	normal-force coefficient
$C_{1/10}$	cycles to damp to 1/10 amplitude
C_0, C_1, b, k	transfer coefficients
$\bar{c}$	mean aerodynamic chord, ft
D	$\frac{d}{dt}$
g	acceleration due to gravity, ft/sec^2
h_p	pressure altitude, ft
I_Y	moment of inertia about Y-axis, slug-ft^2
M	Mach number
m	mass, slugs
n	normal acceleration, g units
P	period, sec
q	dynamic pressure, lb/ft^2

S	wing area, sq ft
$T_{1/2}$	time to damp to one-half amplitude, sec
t	time, sec
V	velocity, ft/sec
α	angle of attack, deg or radians
$\dot{\alpha}$	$\frac{d\alpha}{dt}$
β	sideslip angle, deg
δ_e	average elevon angle, $\frac{\delta_{e_L} + \delta_{e_R}}{2}$, deg
ζ	damping ratio, ratio of damping to critical damping
θ	pitch angle, radians
$\dot{\theta}$	pitch angular velocity, radians/sec
ρ	mass density of air, slugs/ft^2
ϕ	phase angle, deg
ω	frequency, radians/sec
ω_n	undamped natural frequency, radians/sec
C_{L_α}	$dC_L/d\alpha$
$C_{m_{\delta_e}}$	$dC_m/d\delta_e$
C_{m_α}	$dC_m/d\alpha$
$C_{m_{\dot{\theta}}}$	$dC_m \Big/ d\,\frac{\dot{\theta}\bar{c}}{2V}$
$C_{m_{\dot{\alpha}}}$	$dC_m \Big/ d\,\frac{\dot{\alpha}\bar{c}}{2V}$

Subscripts:

L	left
R	right

INSTRUMENTATION

Standard NACA instrumentation was used to record the following quantities: airspeed, altitude, normal acceleration, longitudinal acceleration, transverse acceleration, pitching velocity, rolling velocity, yawing velocity, angle of attack, angle of sideslip, elevon position, and rudder position. All records were synchronized by a common timer at intervals of 0.1 second. An airspeed head, mounted on a boom approximately 5.4 feet ahead of the airplane nose inlet, measured both static and total pressure. Airspeed was calibrated by pacer and radar tracking and the Mach number is believed accurate to ±0.01.

Accelerations and angular velocities were measured by standard NACA direct recording instruments. Control positions were measured by standard control position transmitters and were recorded on a Weston galvanometer. Angle of attack was measured by a vane-type pickup and was also recorded on a Weston galvanometer. The pitching velocity was recorded by an instrument which had a range of ±0.5 radian per second, had a natural frequency of 9.5 cycles per second, and was 0.64 critically damped. The accuracy of the instrument is believed to be ±0.005 radian per second. The normal-accelerometer range was 8g to -1 g. The instrument had a natural frequency of 13.1 cycles per second, was 0.636 critically damped for an altitude of 30,000 feet, and is believed to be accurate to ±0.05g. The recording range of the elevon-control positions was 15° up and 5° down. These control positions are believed to be accurate to $\pm 0.1^{\circ}$.

TEST VEHICLE

The XF-92A is a single-place fighter-type delta-wing airplane. It is powered by a J33-A-29 turbojet engine with afterburner. Physical characteristics are presented in table I and a three-view sketch of the airplane is shown as figure 1. The airplane is controlled by a conventional rudder and by full-span elevons, which function as elevators and ailerons. All control surfaces are operated by an irreversible hydraulic system with artificial feel. Defects in the present hydraulic control system make precise maneuvering of the airplane difficult.

Airplane weights and center-of-gravity positions were determined from pilot reports of fuel remaining. The airplane weight varied from test to test, an average weight being 13,300 pounds. Center-of-gravity position varied with weight from 27.4 percent mean aerodynamic chord to 27.8 percent mean aerodynamic chord.

FLIGHT-TEST MEASUREMENTS

The flight tests for this investigation were conducted in a manner similar to those of reference 4. The airplane was stabilized in 1 g flight at a specified Mach number and altitude and was disturbed by a rapid pulse-type movement of the elevon control. Following the disturbance, all controls were held fixed until the airplane oscillation damped completely. Tests were made with both positive and negative elevon pulses. The direction of input had no effect on the airplane oscillatory characteristics. For the maneuver, about 2° of elevon control gave a maximum airplane response of the order of 2.5g in acceleration and of 0.2 radian per second in pitching velocity. For most tests the amplitudes of these quantities were lower. From the recording of each such maneuver a complete frequency response was computed.

Figure 2 shows representative time histories of the test maneuvers. Presented are normal acceleration, angle of attack, pitching velocity, elevon angle, and sideslip angle. The sideslip angle is presented to emphasize the independence of the longitudinal and directional modes. Little coupling, either aerodynamic or engine gyroscopic, was noted during these maneuvers.

Test data were obtained from 36,000 to 27,000 feet for a Mach number range of 0.42 to 0.94. Figure 3 presents values of angle of attack, normal-force coefficient, and elevon angle prior to the test maneuvers. Test elevon angles are compared to trim values for an altitude of 30,000 feet from reference 2. Actual test altitudes are indicated in table II and on the figures where applicable.

METHODS OF ANALYSIS

Through the cooperative efforts of the Ames and Langley Laboratories, results were obtained by utilizing three methods of analysis (referred to as analysis of the oscillation characteristics, analogue, and Fourier). By measuring the airplane oscillatory characteristics and by analogue simulation, certain airplane stability derivatives may be determined from transient flight data. Since both methods are based on the assumption that two linear differential equations adequately describe the airplane

longitudinally, the results of these analyses compliment each other and may be used to minimize errors in either of the methods. The airplane frequency-response characteristics may be determined from the analogue and Fourier transform analyses and may be compared also. Since all three methods are well known, only a brief description of each method will follow.

Analysis of the Oscillation Characteristics

As was done in reference 1, the period and time to damp were measured directly from the controls-fixed portion of the transient time history. These quantities were combined by the method of reference 5 to give the static stability parameter,

$$C_{m_\alpha} = -\frac{I_Y}{qS\bar{c}}\left[\left(\frac{2\pi}{P}\right)^2 + \left(\frac{0.693}{T_{1/2}}\right)^2\right]$$

By using the lift-curve slope from reference 3 and the rate of oscillation decay, the damping factor $C_{m_{\dot{\theta}}} + C_{m_{\dot{\alpha}}}$ was evaluated as

$$C_{m_{\dot{\theta}}} + C_{m_{\dot{\alpha}}} = \frac{4I_YV}{qS\bar{c}^2}\left(C_{L_\alpha}\frac{\rho SV}{4m} - \frac{0.693}{T_{1/2}}\right)$$

This type of analysis can be used successfully in dealing with lightly damped systems.

Analogue Analysis

This method of analysis (used also in ref. 1) makes use of the Reeves Electronic Analogue Computer to simulate the airplane time-response characteristics. A solution to the transfer-function equation

$$\frac{\dot{\theta}}{\delta_e} = \frac{C_0 + C_1D}{D^2 + bD + k}$$

is obtained by substituting $e^{i\omega t}$ for the operator D. By using the elevon position as an input to the computer, the transfer coefficients C_0, C_1, b, and k are altered until the computed response most nearly duplicates the actual pitching velocity flight record. Shown as figure 4 is a typical example of the match obtained from this type of analysis. This analysis was performed by the Flight Research Branch of the Ames Laboratory. From the transfer coefficients thus evaluated, the control effectiveness, static stability, and damping factor were evaluated by

$$C_{m_{\delta_e}} = - C_1 \frac{I_Y}{qS\bar{c}}$$

$$C_{m_\alpha} = - \frac{kI_Y}{qS\bar{c}}$$

and

$$C_{m_{\dot{\theta}}} + C_{m_{\dot{\alpha}}} = \frac{4I_Y V}{qS\bar{c}^2}\left(\frac{C_{L_\alpha}\rho VS}{4m} - \frac{b}{2}\right)$$

Fourier Analysis

For certain analyses, a system is more conveniently described by its frequency-response characteristics. Computations have been made by applying the Fourier transformation to these same data. The input and output quantities were transformed from the time domain to the frequency domain by the procedure described in reference 4. Such a procedure requires the evaluation of the integrals $\dot{\theta}(i\omega) = \int_0^\infty \dot{\theta}(t)e^{-i\omega t}dt$ and $\delta_e(i\omega) = \int_0^\infty \delta_e(t)e^{-i\omega t}dt$ for the desired frequencies. The results, $\left|\frac{\dot{\theta}}{\delta_e}\right|$ and $\left(\phi_{\dot{\theta}} - \phi_{\delta_e}\right)$, are presented as amplitude ratio $\left|\frac{\dot{\theta}}{\delta_e}\right|$ and phase difference $\phi_{\dot{\theta}} - \phi_{\delta_e}$ as a function of frequency. Also presented are $\left|\frac{n}{\delta_e}\right|$ and $\phi_n - \phi_{\delta_e}$. This procedure requires a vast amount of computation

which is suited to automatic computing methods. This phase of the analysis was computed for the High-Speed Flight Station by the Instrument Research Division data reduction section of the Langley Laboratory.

Some of the major factors that limit the accuracy and reliability of frequency responses calculated from transient flight records are: the time duration of a pulse places a limitation on the frequency range over which reliable transforms can be obtained; the application of a pulse while the airplane is out of trim could result in errors over the entire frequency range; rough air and changes in speed or altitude during a run may affect the frequency response without noticeably distorting the time history; recording instruments with nonlinear dynamic characteristics might seriously affect the high frequency part of airplane response; and random film reading errors may cause spurious high frequency harmonics. Frequency responses obtained with the XF-92A from the recorded transients could be subject to some or all of these errors; however, it is felt that the major source of error would be from the test maneuver itself, since the pilot is unable to maneuver the airplane precisely with the present control system.

RESULTS AND DISCUSSION

The following results have been obtained by applying the methods of analysis described in the previous section. The airplane oscillatory characteristics, transfer coefficients, stability derivatives, and frequency-response characteristics as affected by Mach number are discussed herein. Table II summarizes these data. Where practical, data have been corrected to 30,000 feet or, as with the frequency-response plots, the actual test altitude is noted.

Oscillatory Characteristics

Results of the measurement of the oscillatory characteristics are shown as figure 5. For an altitude of 30,000 feet, the airplane period and time to damp to one-half amplitude decreased with increasing Mach number. Up to a Mach number of about 0.85, two cycles are required for the airplane oscillation to damp to 1/10 of its initial value. At about $M = 0.93$, three cycles are required. The airplane does not meet the Air Force handling-qualities requirement that the longitudinal short-period oscillation damp to 1/10 amplitude in one cycle at any Mach number. Shown also are the results of reference 1. Agreement is satisfactory considering that the data of reference 1 were obtained from maneuvers not performed to yield this type of information. Discrepancies in the results of the two investigations are probably due to small control motions giving

the illusion of lower damping for the referenced data. The data of figure 5 are converted to undamped natural frequency and damping ratio and are presented as figure 6.

Transfer Coefficients

A summary of the results of the analogue computer analysis in the form of transfer coefficients C_0, C_1, b, and k, is presented in table II. Inasmuch as these data were not obtained at the same test altitude, they were corrected to 30,000 feet by the method suggested in reference 4. These corrected data are presented in figure 7 as a function of Mach number. Wherever possible the period and time-to-damp data were converted to this form and are included in the figure.

Stability Derivatives

As has been shown in references 1, 4, 5, and in many other sources, certain stability derivatives may be determined from the airplane oscillatory characteristics and from transfer coefficients. The static stability C_{m_α} and elevon effectiveness $C_{m_{\delta_e}}$ were computed from the airplane period, time to damp, and the transfer coefficients and are presented as figure 8(a). Over the lower Mach number range a gradual increase in C_{m_α} with Mach number is shown, but the parameter increases by a factor of 2 from $M = 0.75$ to 0.94. The control effectiveness shows little Mach number effect, increasing slightly with Mach number for the range of these tests. Comparison is made with the results of references 1 and 6 and with full-scale tests in the Ames 40- by 80-foot wind tunnel. Figure 8(b) shows the airplane damping factor and also the airplane lift-curve slope (from ref. 3) used in computing the factor. This parameter has a value of about -1.0 over most of the test Mach number range. These data are compared with results of reference 1 and with tunnel tests of a 63° delta-wing model with an aspect ratio of 2 (ref. 7) with reasonable agreement.

Frequency-Response Characteristics

Representative data were selected and analyzed by the Fourier transform method to give the frequency-response characteristics of the airplane for the range of these tests. Results of these computations, corrected for instrument characteristics, are presented in figures 9 and 10 in the typical form of amplitude ratio $\left|\frac{\dot{\theta}}{\delta_e}\right|$ and $\left|\frac{n}{\delta_e}\right|$ and phase angle $\phi_{\dot{\theta}/\delta_e}$ and ϕ_{n/δ_e} as a function of frequency. Test Mach number

and altitude are presented on each figure. Frequency-response calculations from the transfer coefficients obtained by analogue analysis are compared with the Fourier analysis results.

It can be seen that a second order transfer function adequately describes the airplane over a limited frequency range but at higher frequency differences may be noted in the phase angles. This may be the influence of high frequency airplane modes or may be due to poor accuracy in computing the frequency response at the higher frequencies. Since some uncertainty in the phase angles does exist, fairings of the phase angles presented in figures 9 and 10 are omitted beyond 8 radians per second.

Summary plots of these data are presented as figure 11 and show the trends of amplitude ratio and natural frequency with Mach number.

CONCLUDING REMARKS

Results of dynamic longitudinal flight tests conducted with the XF-92A delta-wing airplane over a Mach number range of 0.42 to 0.94 at about 30,000 feet are presented. These data were analyzed by measuring the airplane oscillatory characteristics, by using an analogue computer to simulate the airplane system, and by determining the frequency response characteristics of the airplane.

For an altitude of 30,000 feet, the airplane period and time to damp decreased with increasing Mach number for the range of these tests. The airplane required 2 cycles to damp to 1/10 amplitude over most of the test range but required 3 cycles at the higher test Mach number. Control effectiveness $C_{m_{\delta_e}}$ was essentially constant throughout the Mach number range of these tests. The static stability C_{m_α} increased with Mach number approximately twofold between Mach numbers of 0.75 and 0.94. The damping factor was essentially constant at about -1.0.

Little coupling, either aerodynamic or engine gyroscopic, was noted during these longitudinal tests.

High-Speed Flight Station,
National Advisory Committee for Aeronautics,
Edwards, Calif., October 7, 1954.

REFERENCES

1. Holleman, Euclid C., Evans, John H., and Triplett, William C.: Preliminary Flight Measurements of the Dynamic Longitudinal Stability Characteristics of the Convair XF-92A Delta-Wing Airplane. NACA RM L53E14, 1953.

2. Sisk, Thomas R., and Mooney, John M.: Preliminary Measurements of Static Longitudinal Stability and Trim for the XF-92A Delta-Wing Research Airplane in Subsonic and Transonic Flight. NACA RM L53B06, 1953.

3. Bellman, Donald R., and Sisk, Thomas R.: Preliminary Drag Measurements of the Consolidated Vultee XF-92A Delta-Wing Airplane in Flight Tests to a Mach Number of 1.01. NACA RM L53J23, 1954.

4. Triplett, William C., and Smith, G. Allan: Longitudinal Frequency-Response Characteristics of a 35° Swept-Wing Airplane As Determined From Flight Measurements, Including a Method for the Evaluation of Transfer Functions. NACA RM A51G27, 1951.

5. Gillis, Clarence L., Peck, Robert F., and Vitale, A. James: Preliminary Results From a Free-Flight Investigation at Transonic and Supersonic Speeds of the Longitudinal Stability and Control Characteristics of an Airplane Configuration With a Thin Straight Wing of Aspect Ratio 3. NACA RM L9K25a, 1950.

6. Stephenson, Jack D., and Amuedo, Arthur R.: Tests of a Triangular Wing of Aspect Ratio 2 in the Ames 12-Foot Pressure Wind Tunnel. II - The Effectiveness and Hinge Moments of a Constant-Chord Plain Flap. NACA RM A8E03, 1948.

7. Tobak, Murray: Damping in Pitch of Low-Aspect-Ratio Wings at Subsonic and Supersonic Speeds. NACA RM A52L04a, 1953.

TABLE I

PHYSICAL CHARACTERISTICS OF THE XF-92A AIRPLANE

Wing:	
Area, sq ft	425
Span, ft	31.33
Airfoil section	NACA 65(06)-006.5
Mean aerodynamic chord, ft	18.09
Aspect ratio	2.31
Root chord, ft	27.13
Tip chord	0
Taper ratio	0
Sweepback (leading edge), deg	60
Incidence, deg	0
Dihedral (chord plane), deg	0
Elevons:	
Area (total, both, aft of hinge line) sq ft	76.19
Span (one elevon), ft	13.35
Chord (aft of hinge line, constant except at tip), ft	3.05
Movement, deg	
Elevator:	
Up	15
Down	5
Aileron, total	10
Operation	Hydraulic
Vertical tail:	
Area, sq ft	75.35
Height, above fuselage center line, ft	11.50
Rudder:	
Area, sq ft	15.53
Span, ft	9.22
Travel, deg	±8.5
Operation	Hydraulic
Fuselage:	
Length, ft	42.80
Power plant:	
Engine	Allison J33-A-29 with afterburner
Rating:	
Static thrust at sea level, lb	5,600
Static thrust at sea level with afterburner, lb	7,500
Weight:	
Gross weight (560 gal fuel), lb	15,560
Empty weight, lb	11,808
Center-of-gravity locations:	
Gross weight (560 gal fuel), percent M.A.C.	25.5
Empty weight, percent M.A.C.	29.2
Moment of inertia in pitch, slug-ft^2	35,000

TABLE II

SUMMARY OF XF-92A TEST DATA

Mach number, M	Altitude, h_p, ft	Period, P, sec	Time to damp, $T_{1/2}$, sec	Transfer coefficients REAC			
				C_0	C_1	b	k
0.420	30.8×10^3	3.30	2.00	----	----	----	----
.425	30.0	3.30	2.10	----	----	----	----
.470	31.6	3.35	2.15	----	----	----	----
.470	31.1	3.35	2.12	----	----	----	----
.490	30.0	2.95	1.65	0	12.1	1.04	4.64
.540	30.0	2.80	1.27	8.8	13.2	1.00	6.06
.590	31.0	2.50	1.47	16.0	17.2	1.24	7.36
.635	29.8	2.20	1.45	----	----	----	----
.640	30.0	2.20	1.26	----	----	----	----
.720	31.0	1.90	1.06	24.8	26.0	1.52	11.4
.740	29.3	1.80	1.07	----	----	----	----
.740	29.2	1.80	.98	----	----	----	----
.765	31.5	1.75	.89	21.8	30.8	1.52	12.8
.770	31.0	1.75	.88	22.1	31.2	1.60	13.8
.840	28.0	1.30	.79	----	----	----	----
.855	27.6	1.30	.79	----	----	----	----
.880	29.5	1.14	.74	----	----	----	----
.880	28.6	1.20	.85	----	----	----	----
.890	27.9	1.10	.75	----	----	----	----
.890	30.0	1.10	.66	----	----	----	----
.910	27.0	.96	.77	68.6	54.4	2.12	41.6
.930	36.5	1.15	1.23	56.0	32.3	1.20	28.5
.935	36.0	1.15	1.23	----	----	----	----
.945	32.0	1.04	.85	16.0	44.5	1.68	35.2

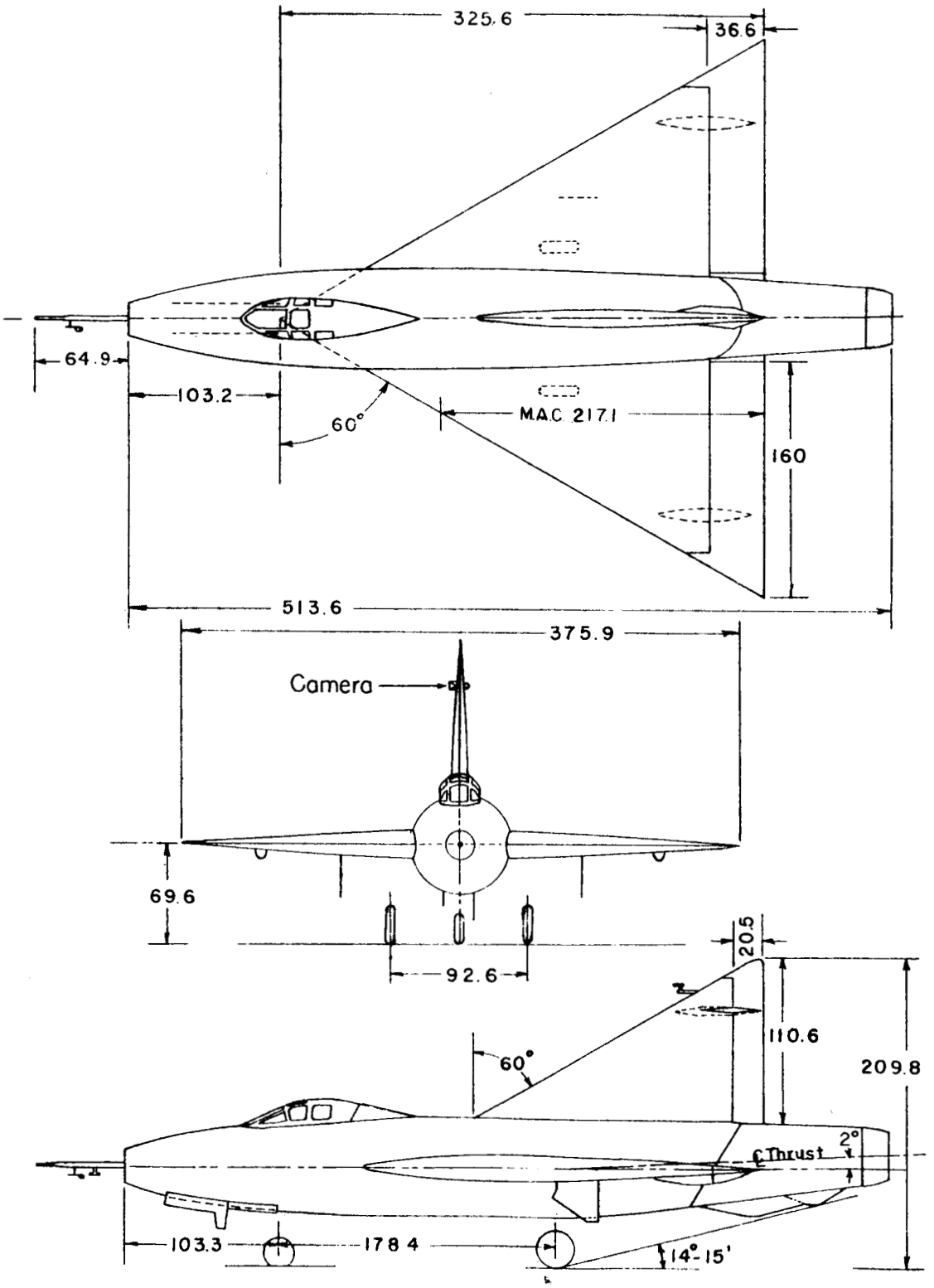

Figure 1.- Three-view drawing of XF-92A airplane.

[redacted]

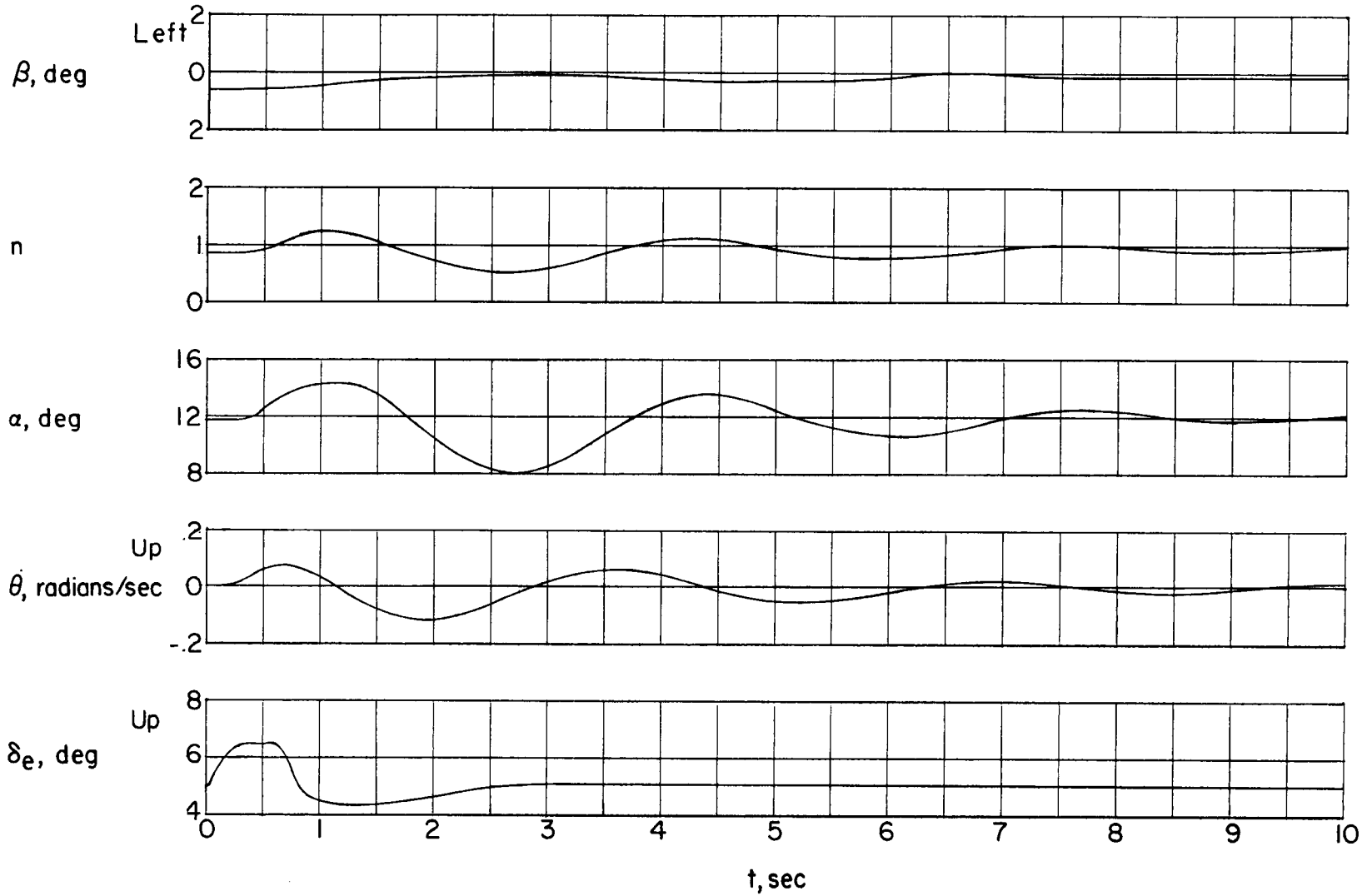

(a) M = 0.420; h_p = 30,800 feet.

Figure 2.- Representative time histories of the test maneuver.

[redacted]

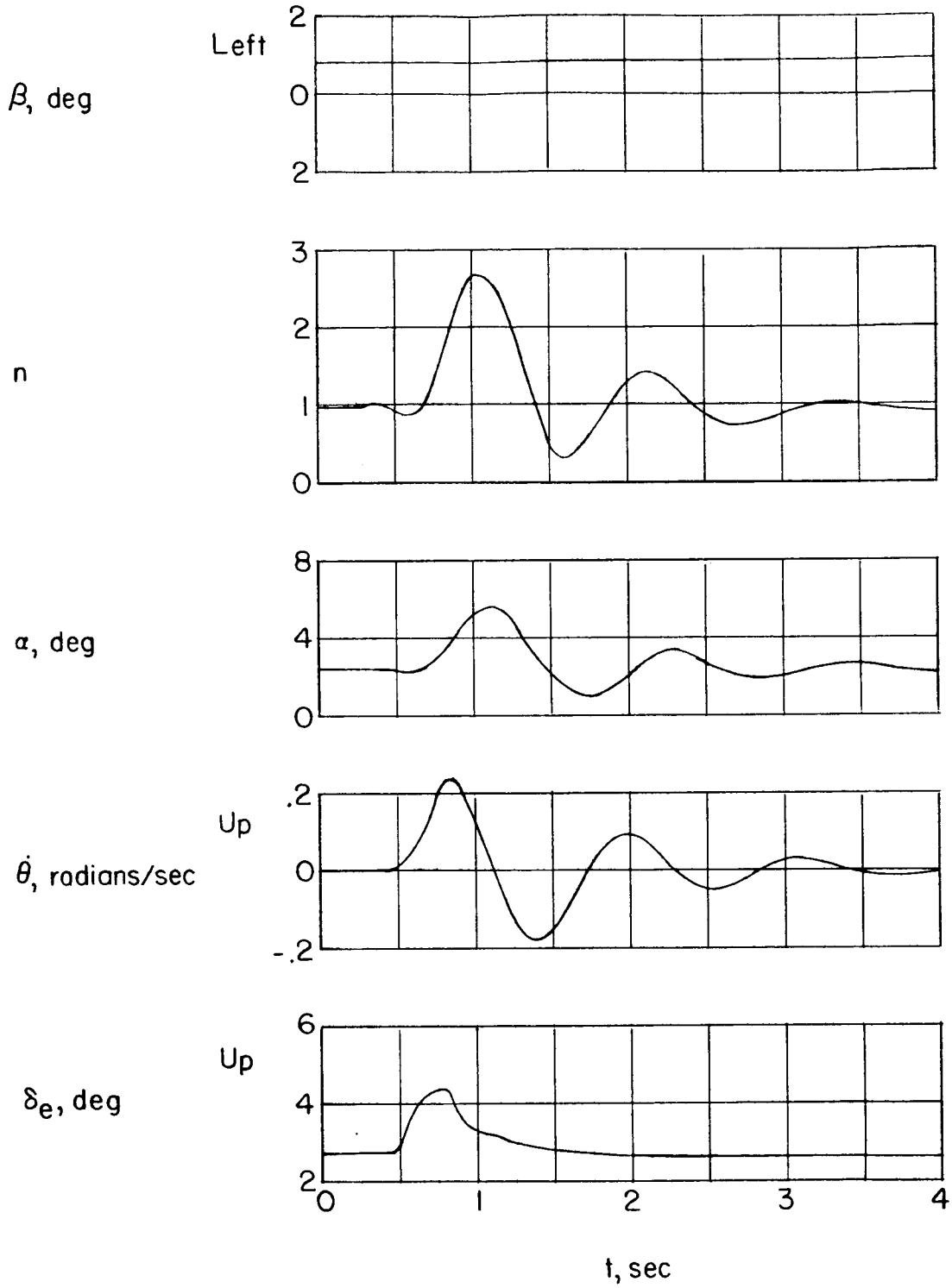

(b) M = 0.890; h_p = 30,000 feet.

Figure 2.- Continued.

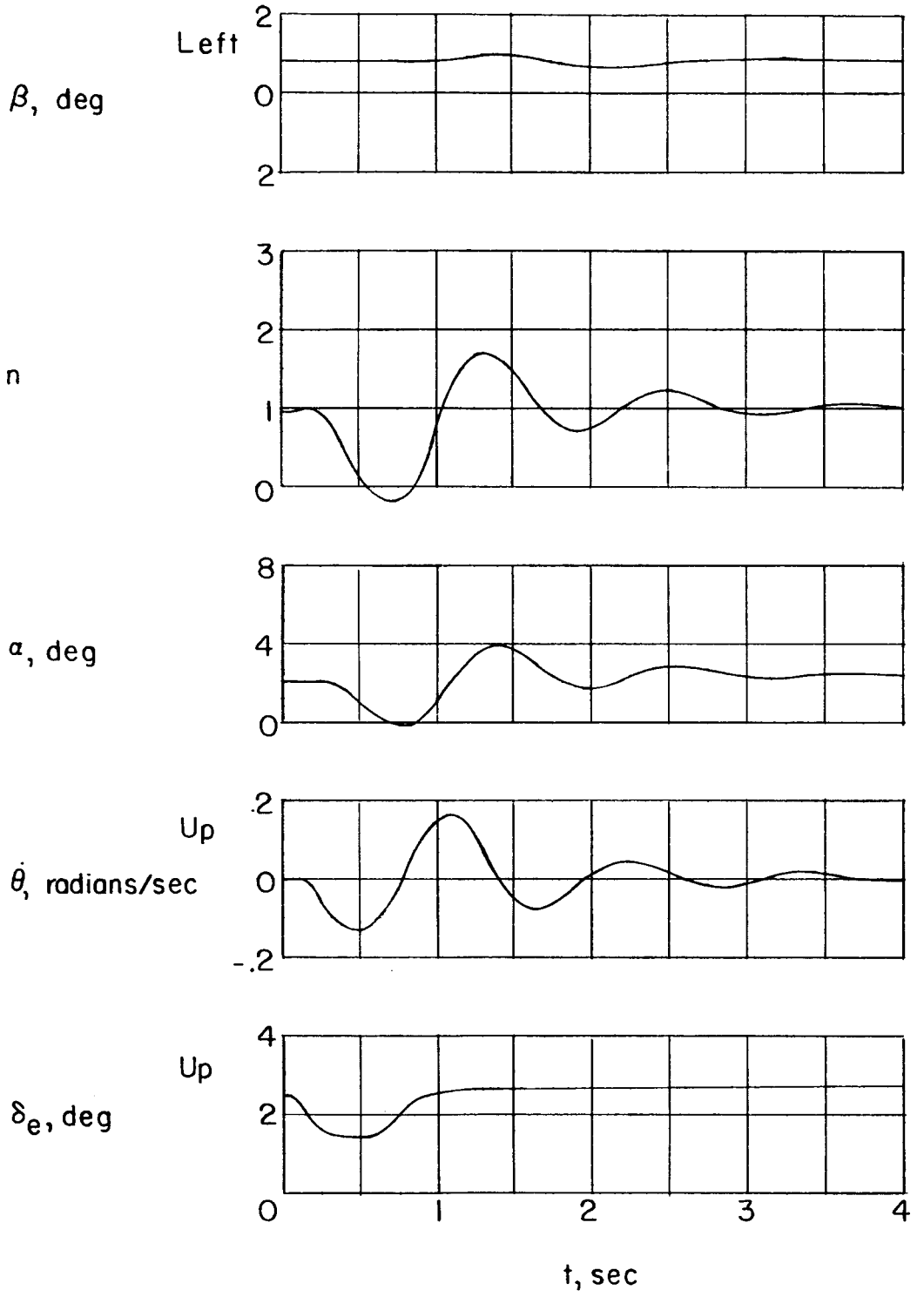

(c) M = 0.880; h_p = 29,500 feet.

Figure 2.- Concluded.

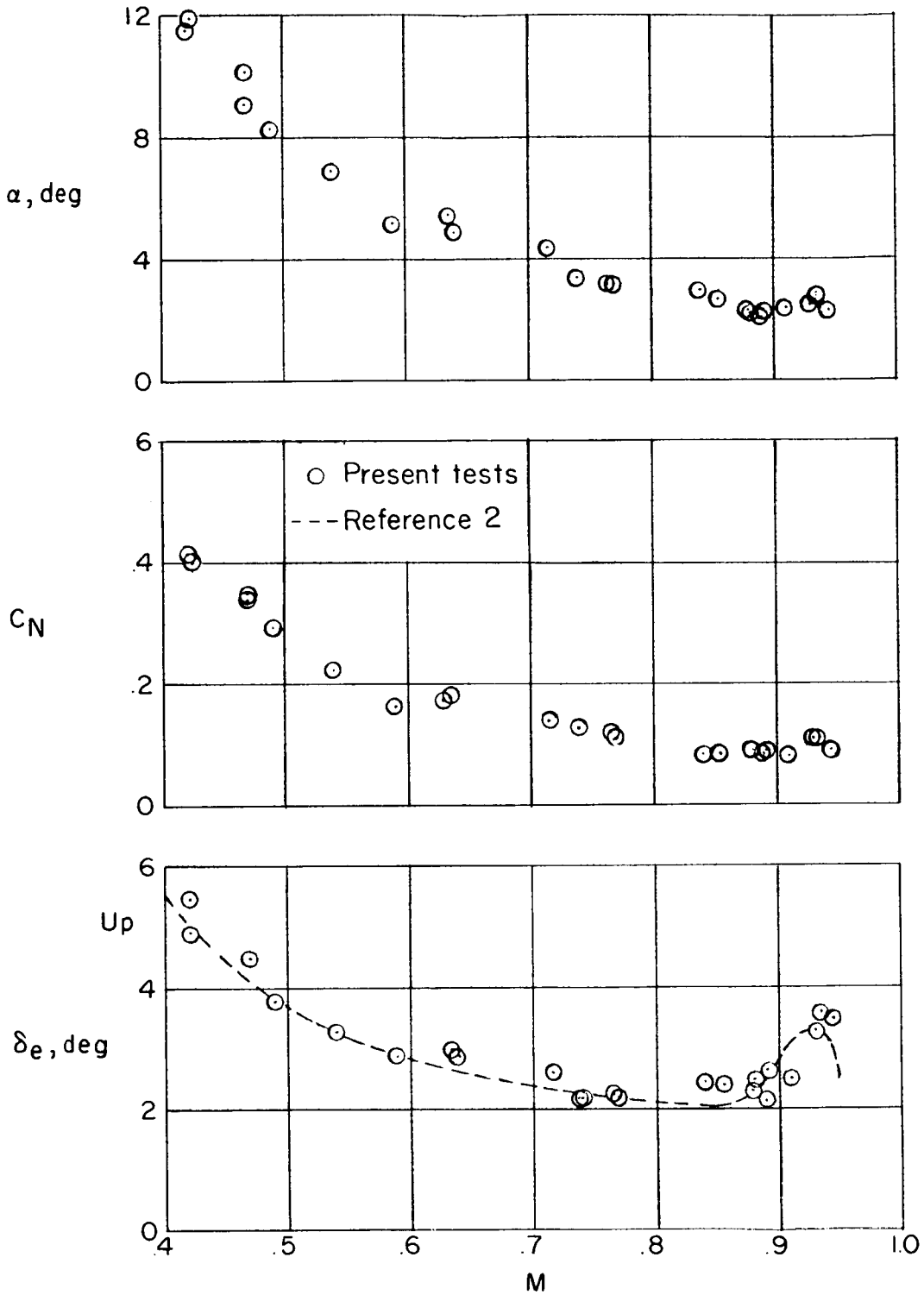

Figure 3.- Variation of trim angle of attack, normal-force coefficient, and control angle with Mach number.

[redacted]

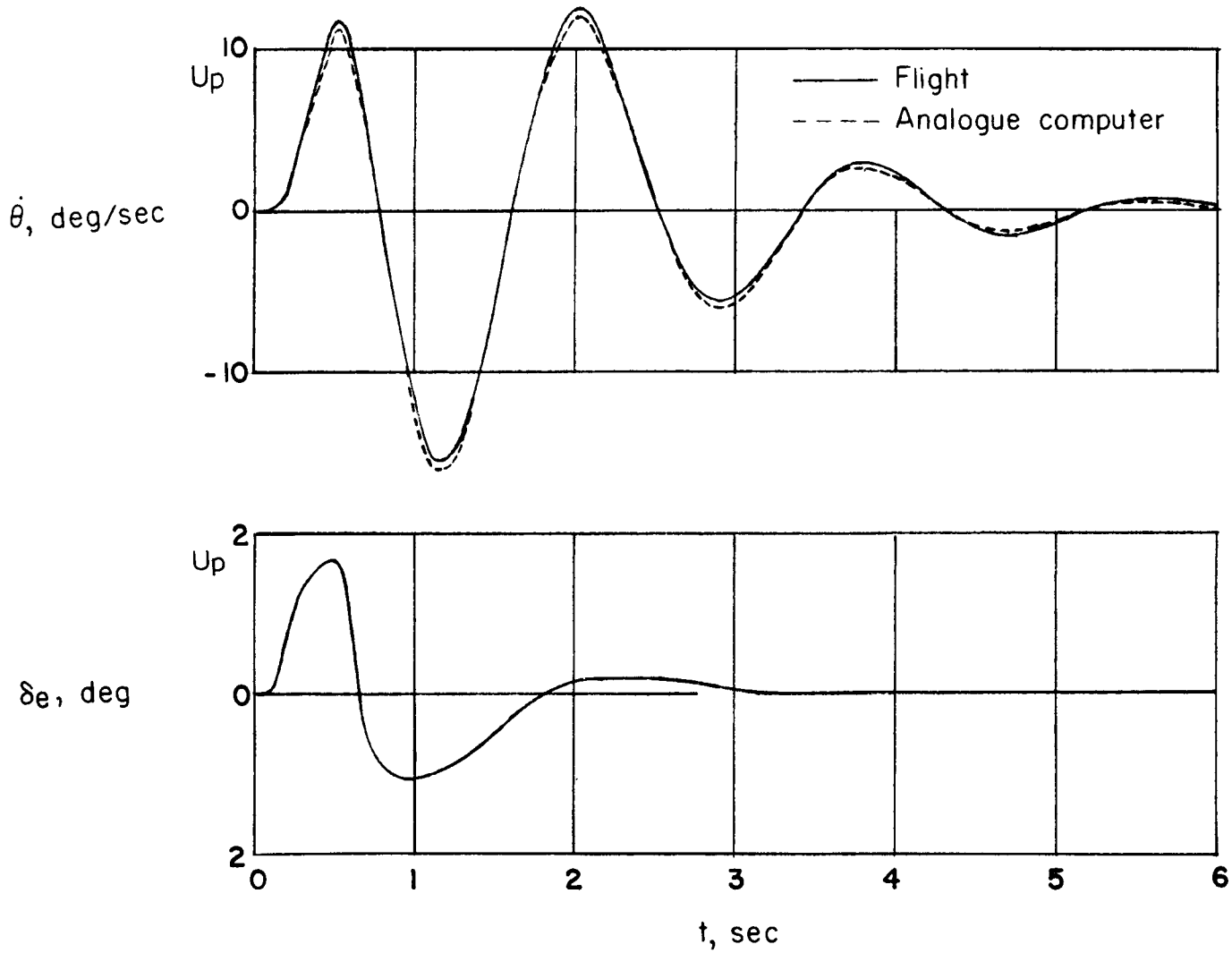

Figure 4.- Example of the analogue computer solution compared to the actual flight record. M = 0.77.

[redacted]

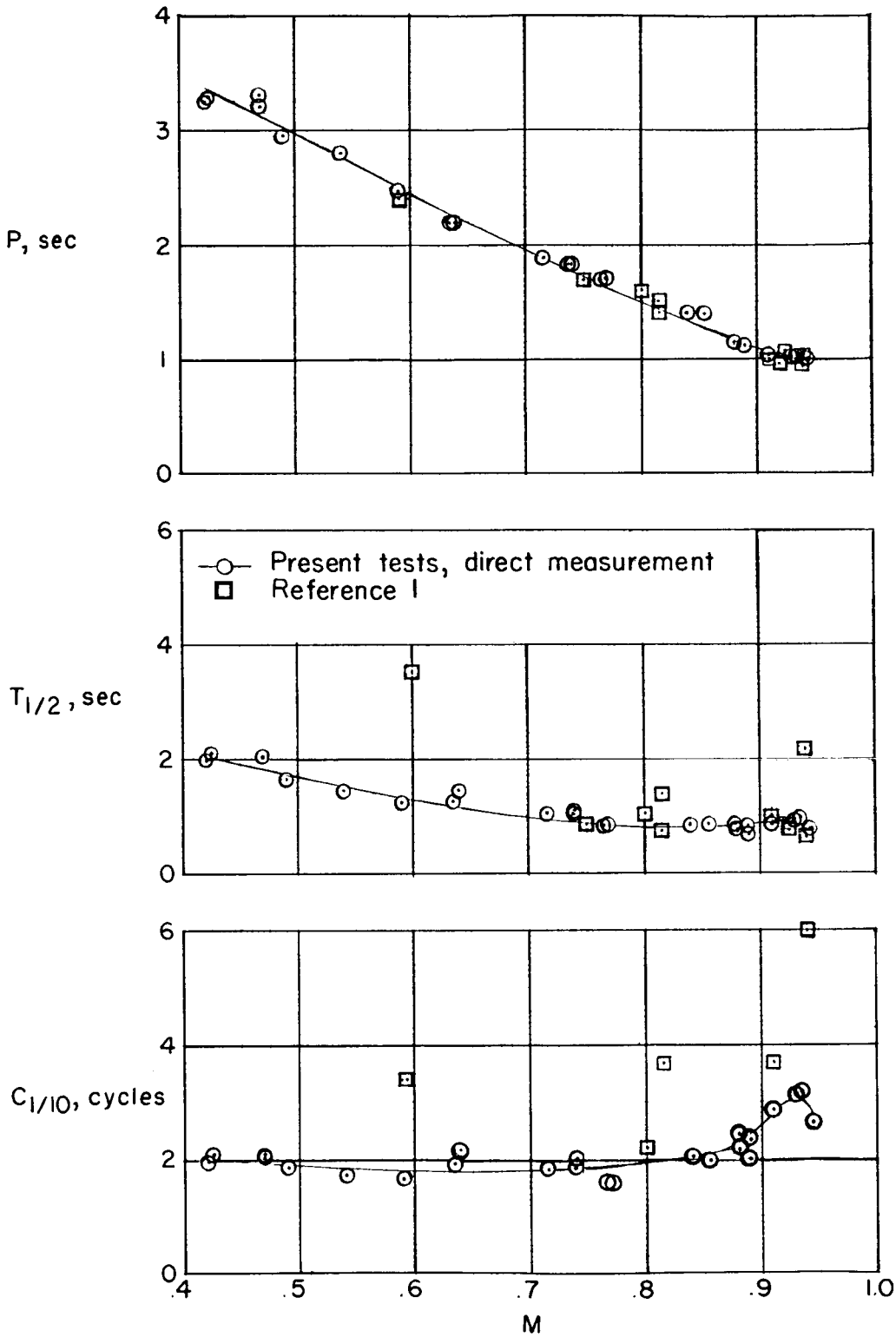

Figure 5.- Variation of the airplane oscillatory characteristics with Mach number for a test altitude of 30,000 feet.

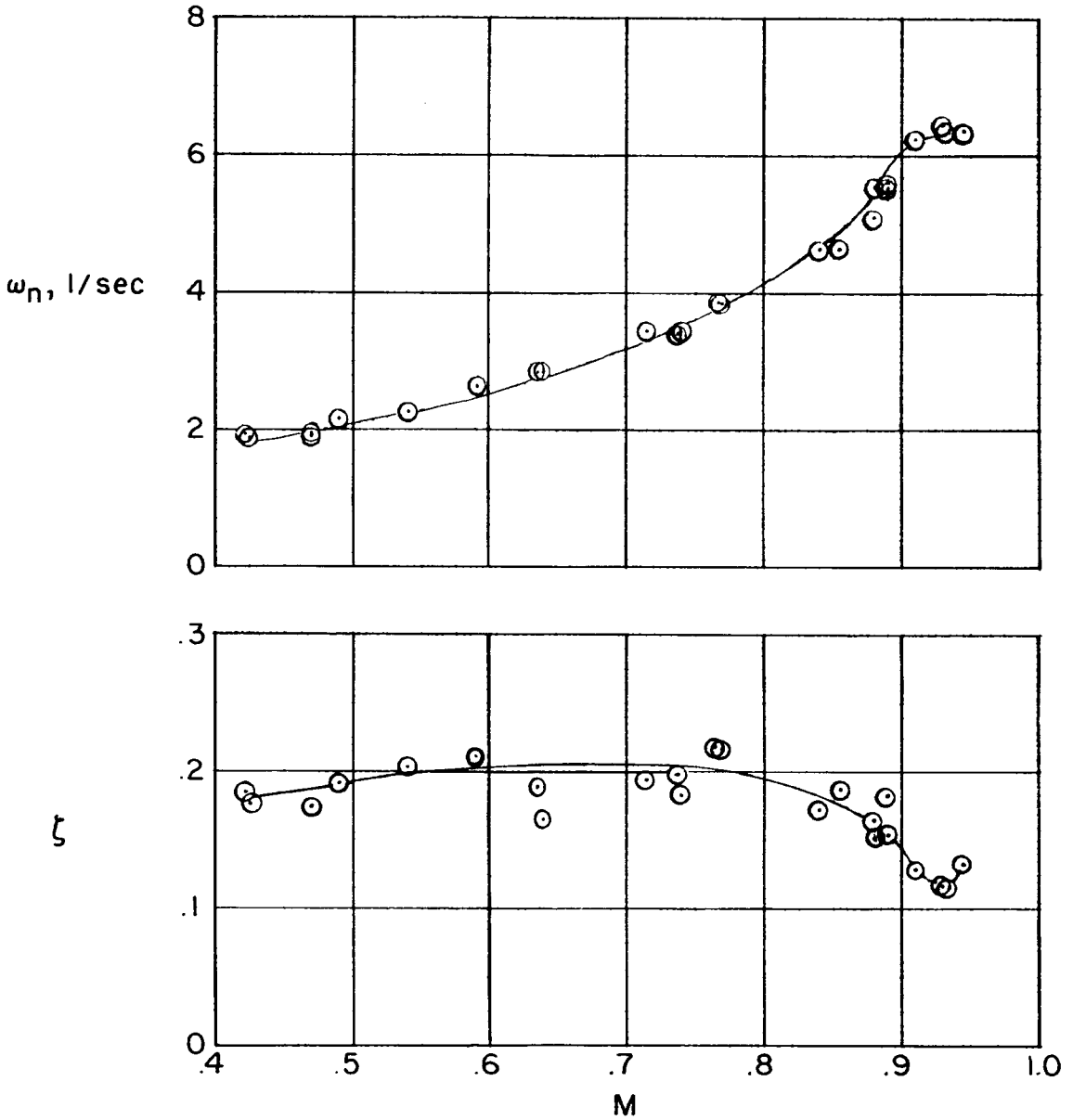

Figure 6.- Variation of undamped natural frequency and damping ratio with Mach number for a test altitude of 30,000 feet.

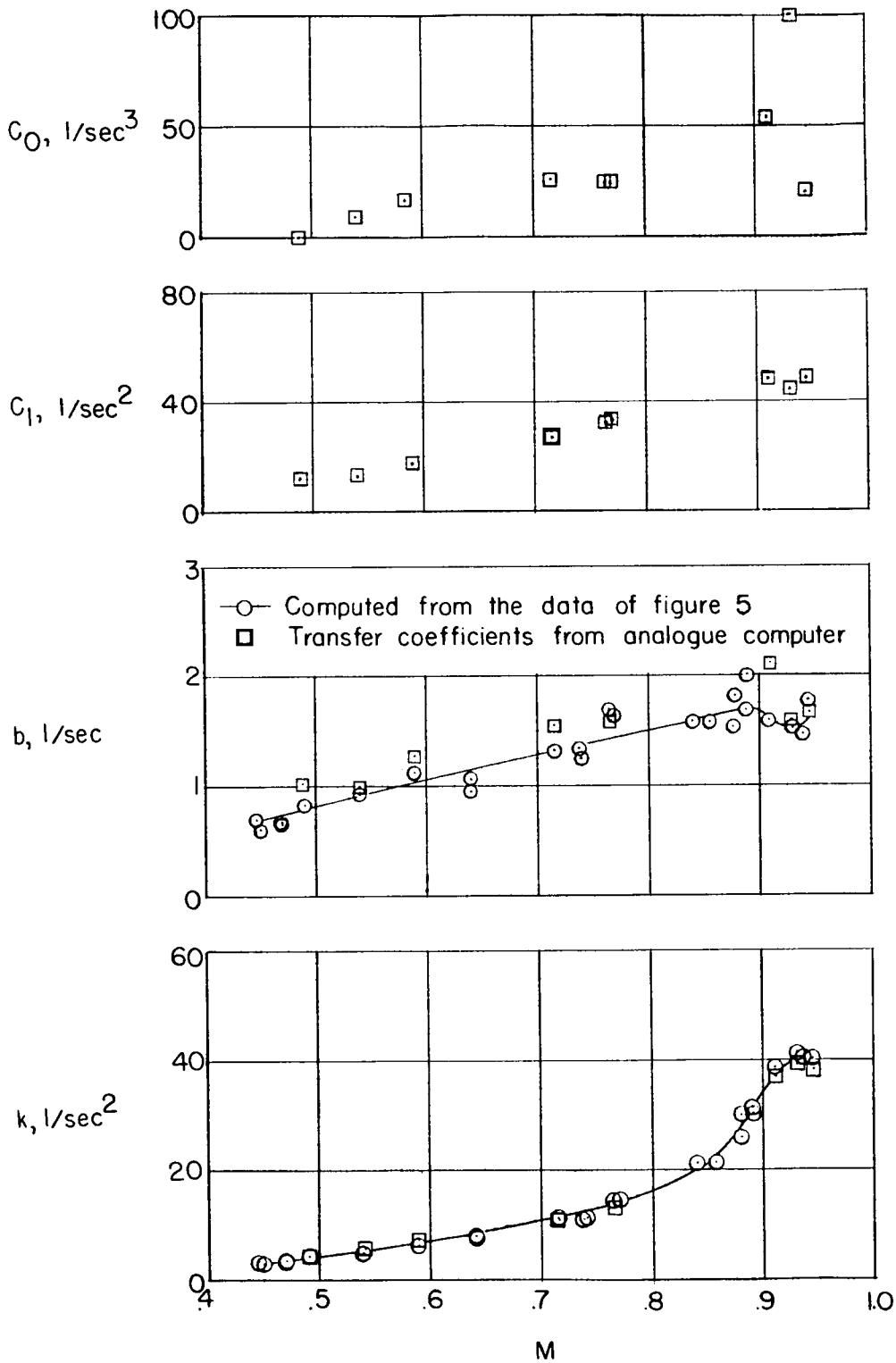

Figure 7.- Variation of transfer coefficients with Mach number for a test altitude of 30,000 feet.

[redacted]

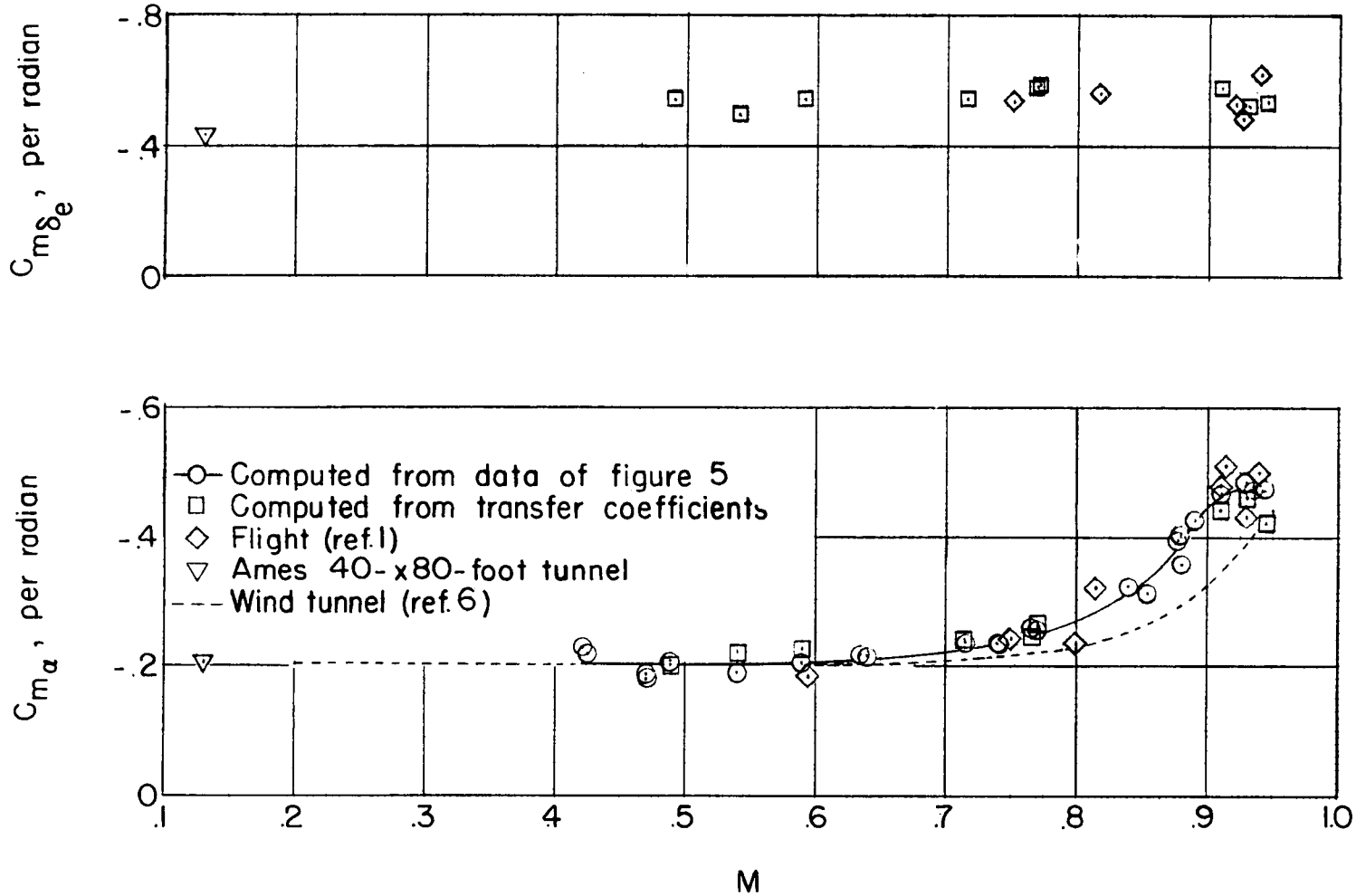

(a) Control effectiveness and static stability.

Figure 8.- Variation of stability derivatives with Mach number.

[redacted]

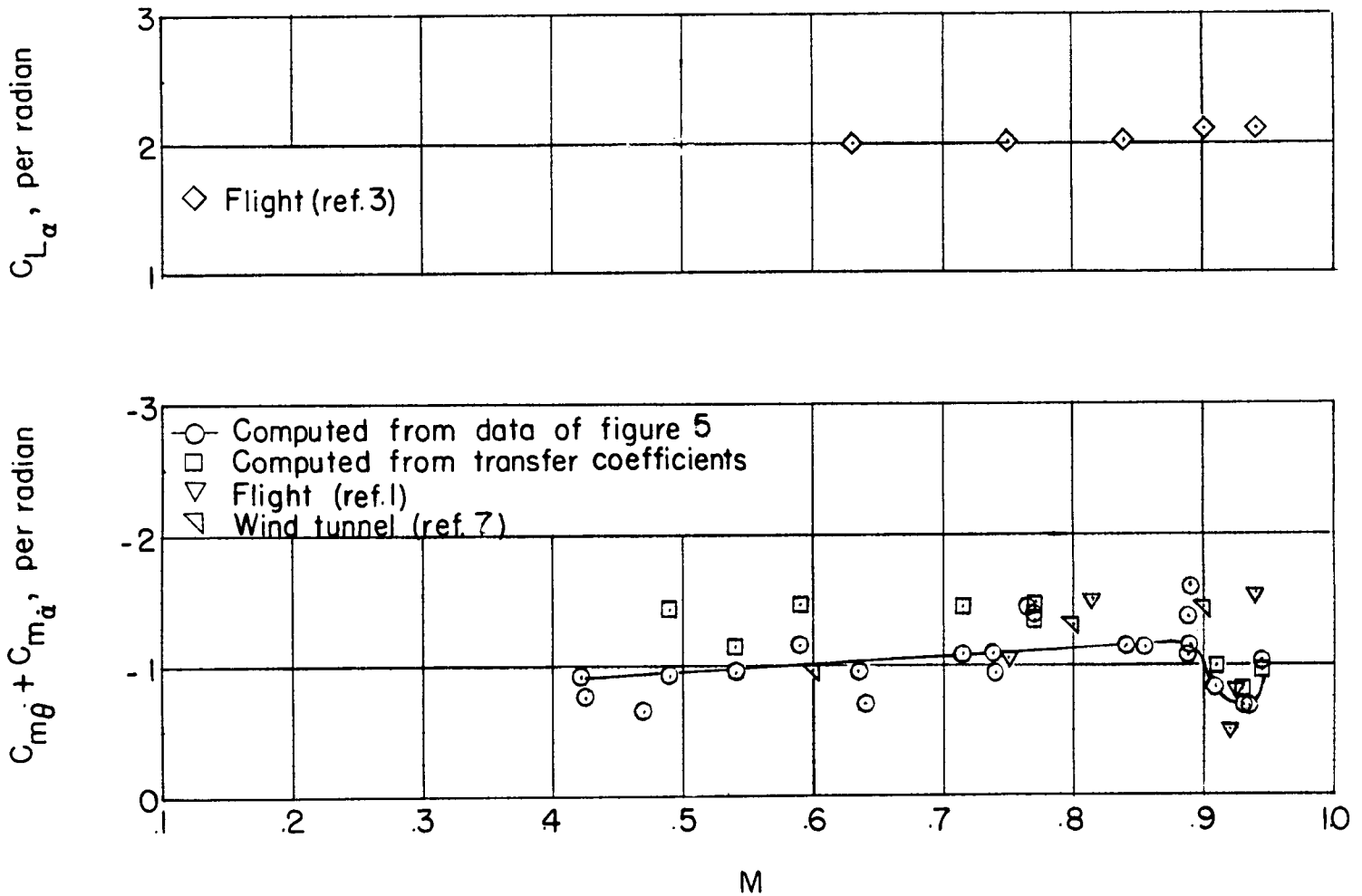

(b) Damping factor.

Figure 8.- Concluded.

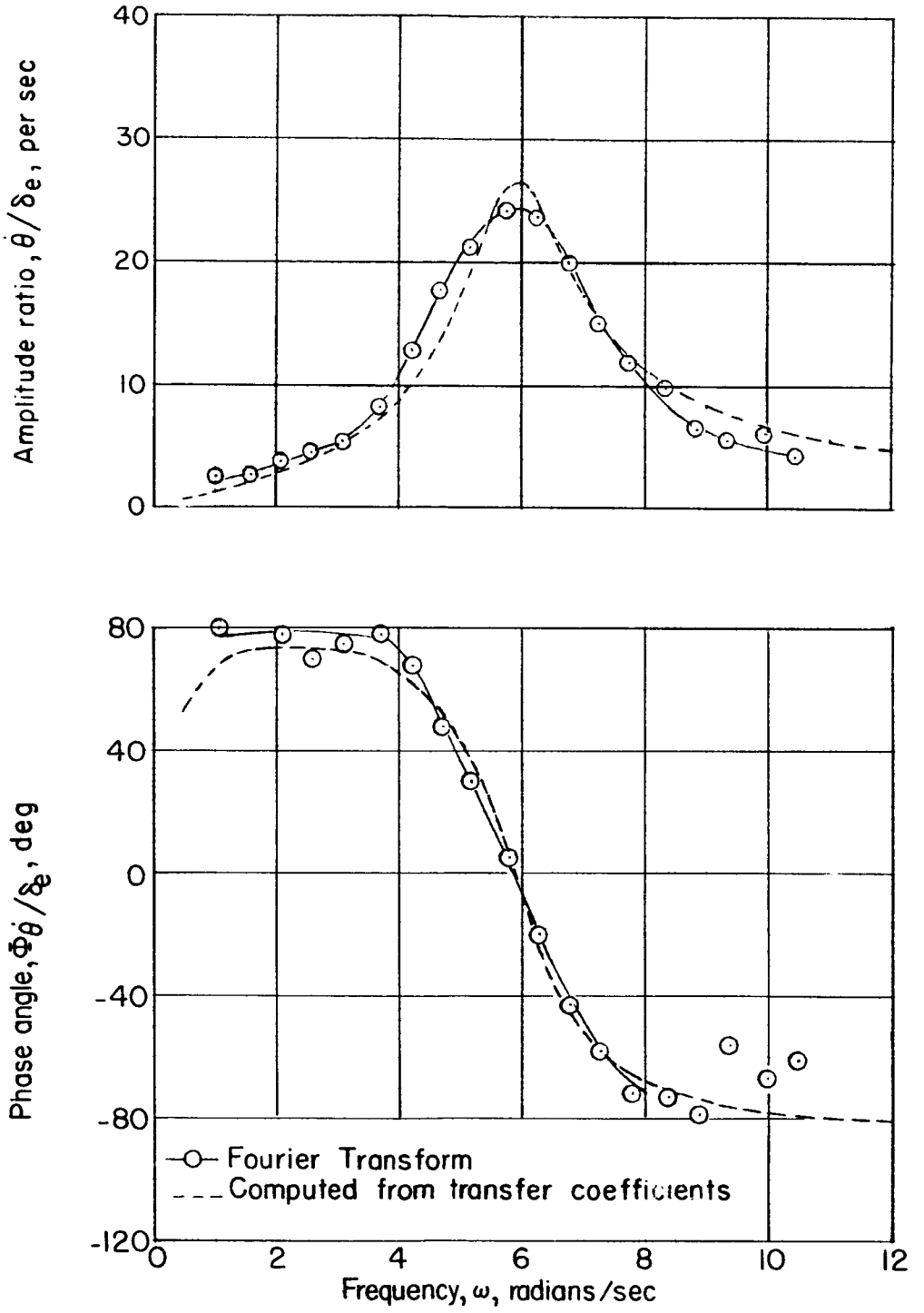

(a) M = 0.945; h_p = 32,000 feet.

Figure 9.- Pitching velocity frequency response characteristics for various Mach numbers.

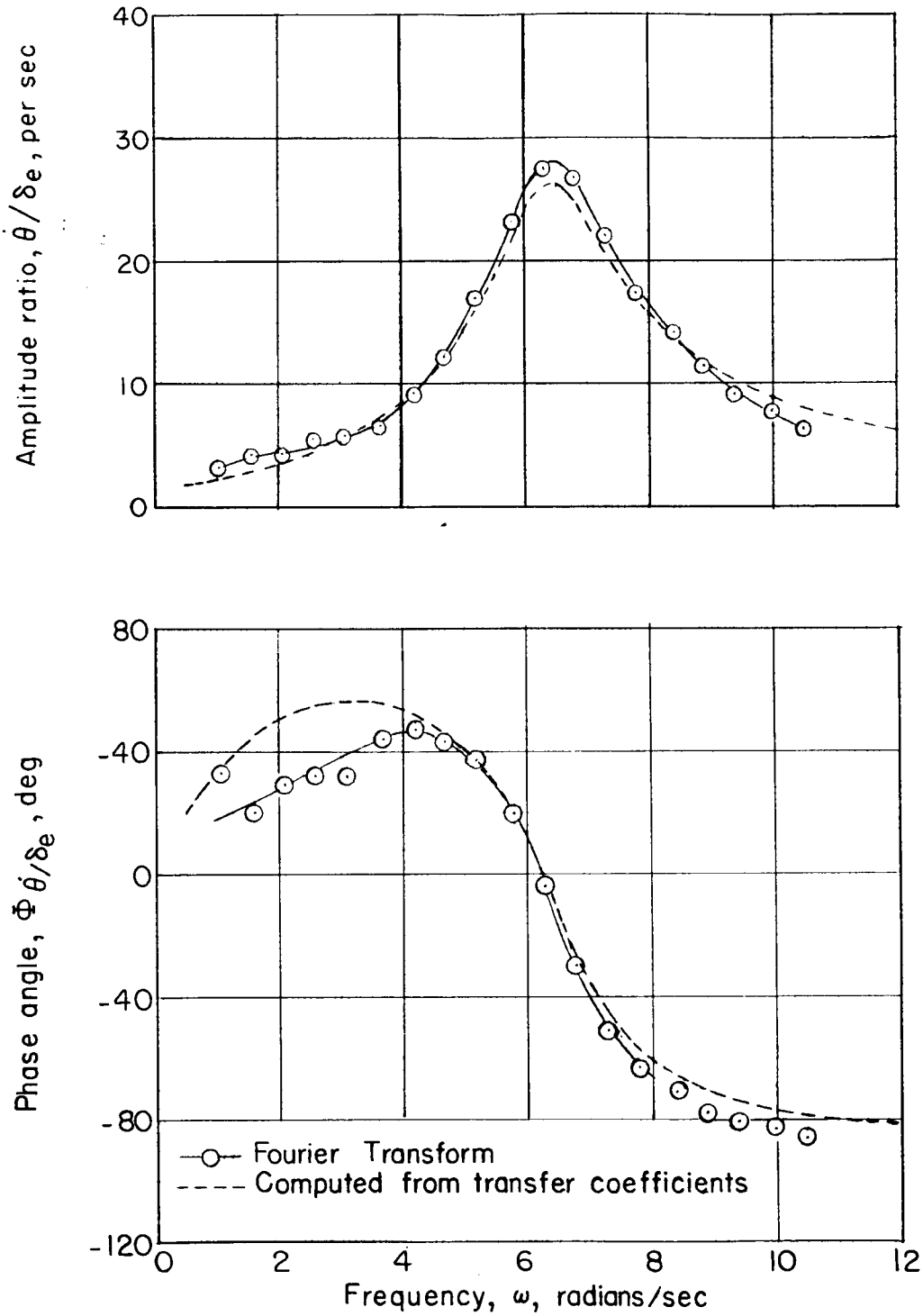

(b) M = 0.910; h_p = 27,000 feet.

Figure 9.- Continued.

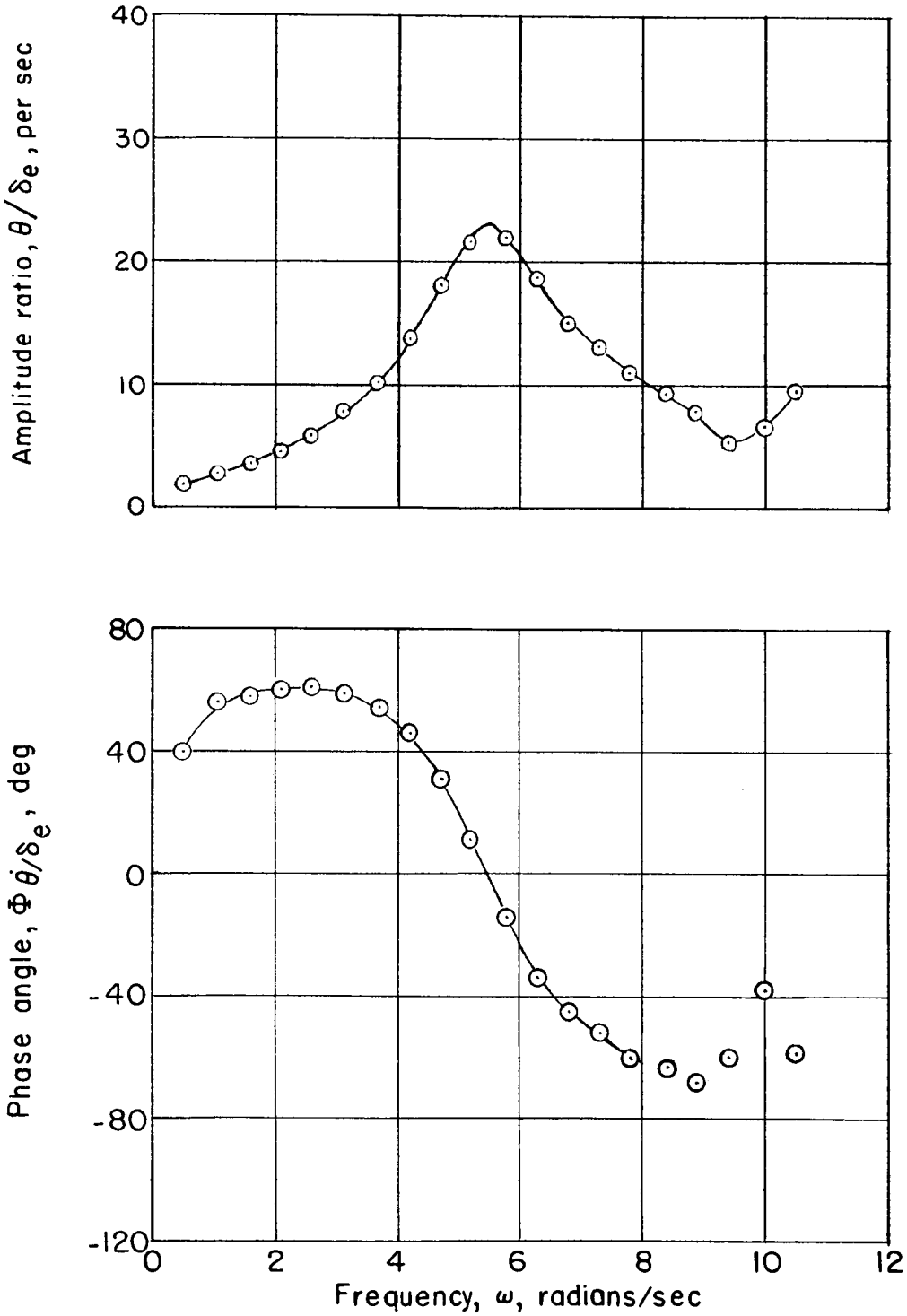

(c) M = 0.890; h_p = 30,000 feet.

Figure 9.- Continued.

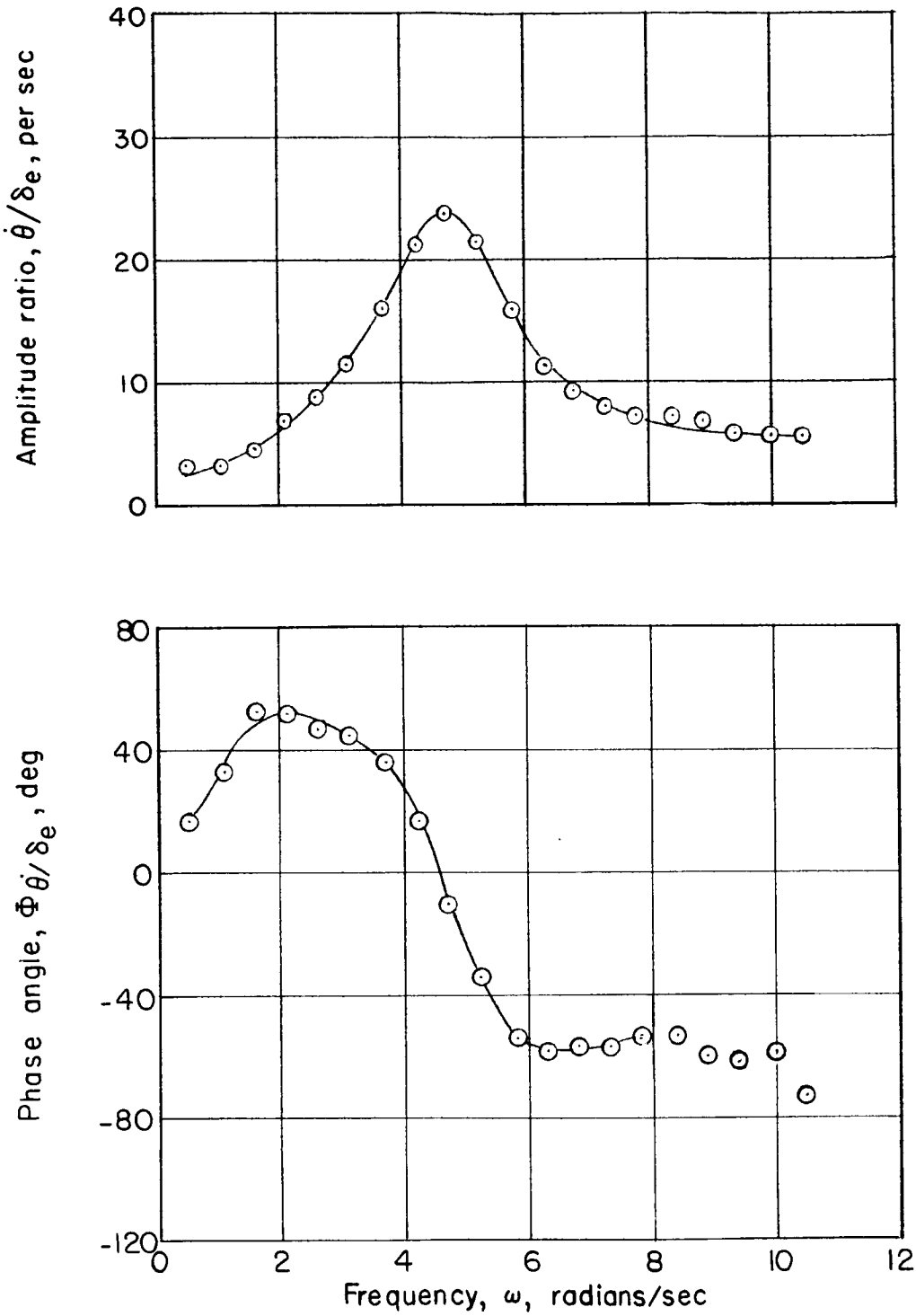

(d) M = 0.840; h_p = 28,000 feet.

Figure 9.- Continued.

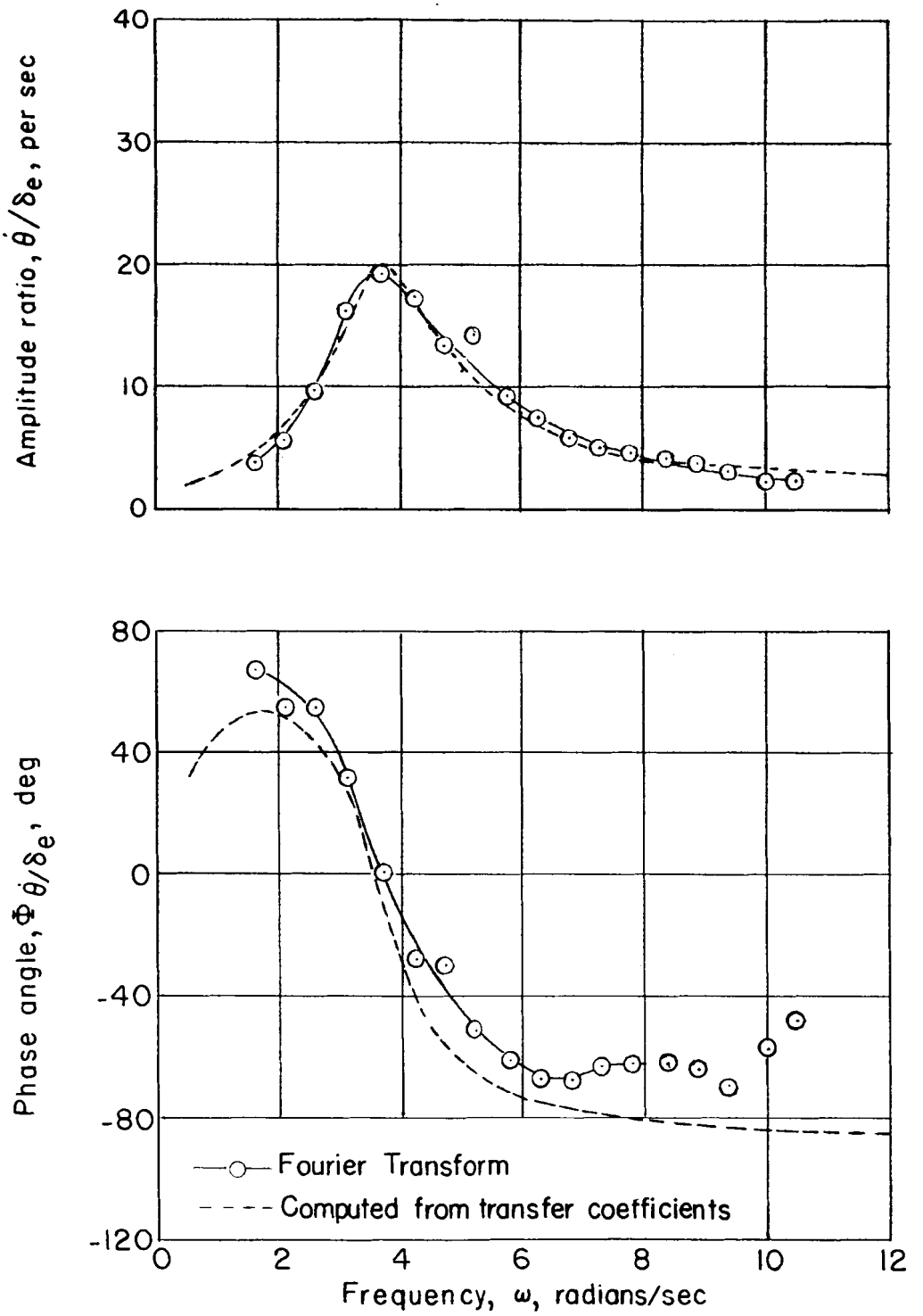

(e) M = 0.770; h_p = 31,000 feet.

Figure 9.- Continued.

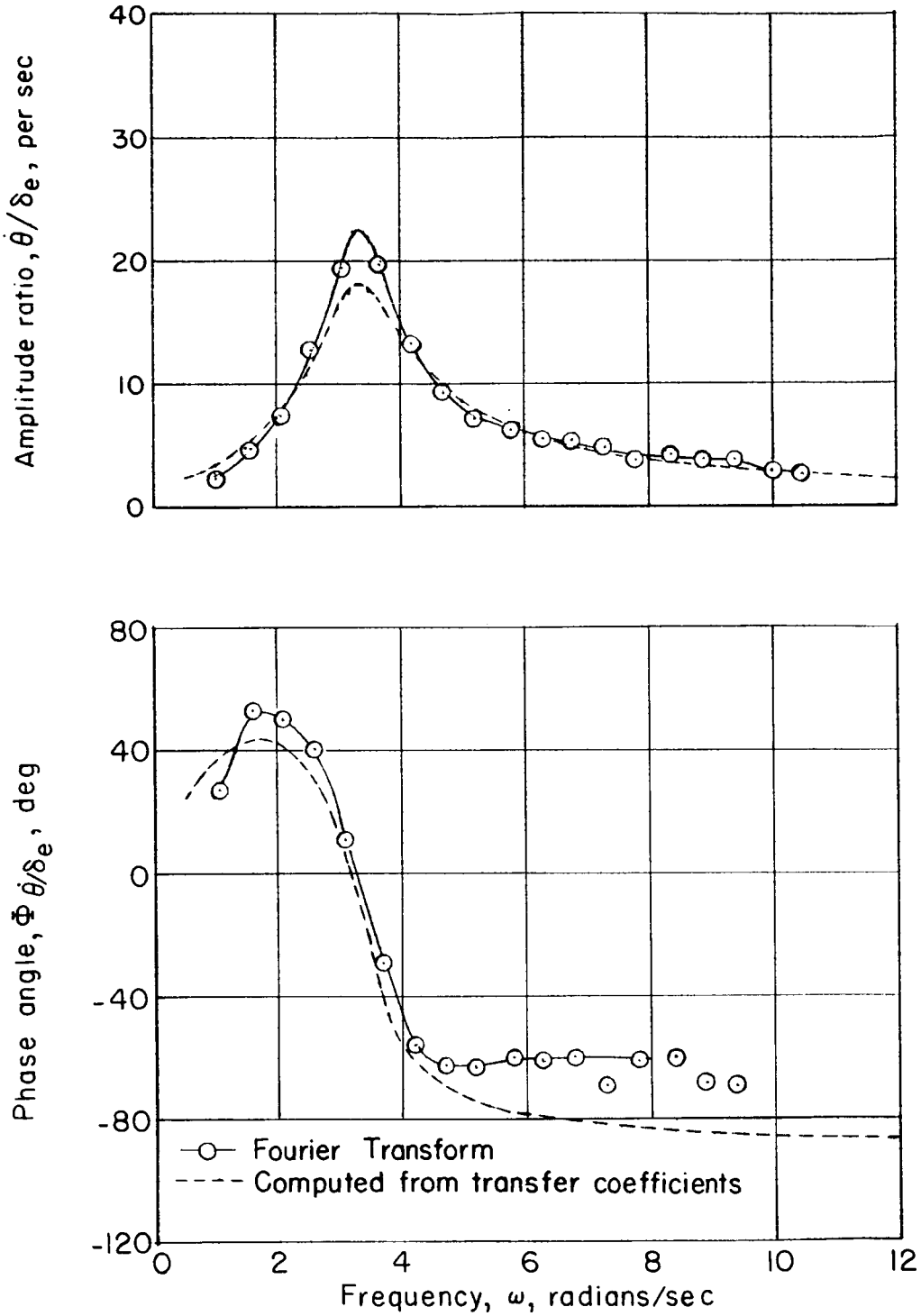

(f) M = 0.720; h_p = 31,000 feet.

Figure 9.- Continued.

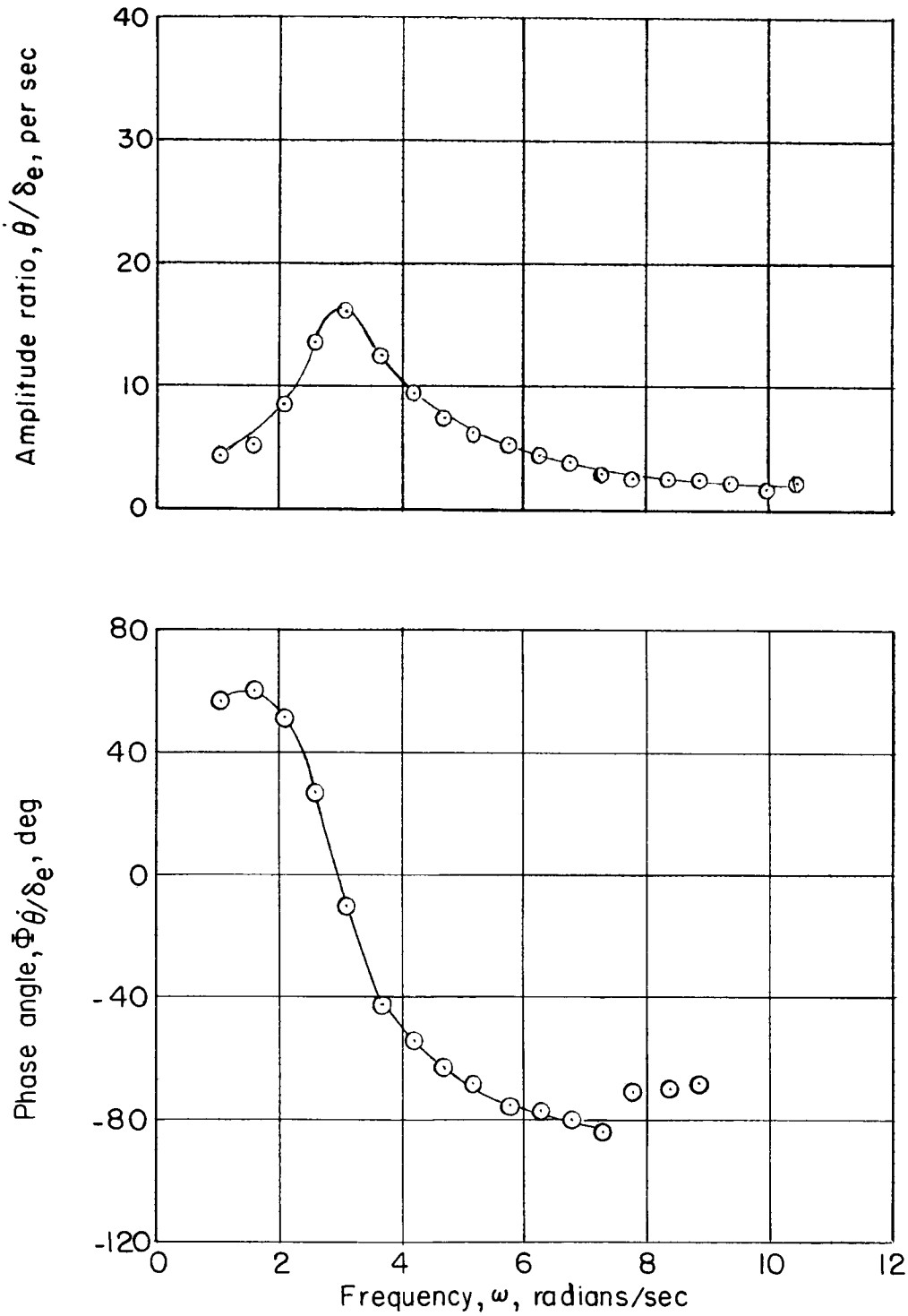

(g) M = 0.640; h_p = 30,000 feet.

Figure 9.- Continued.

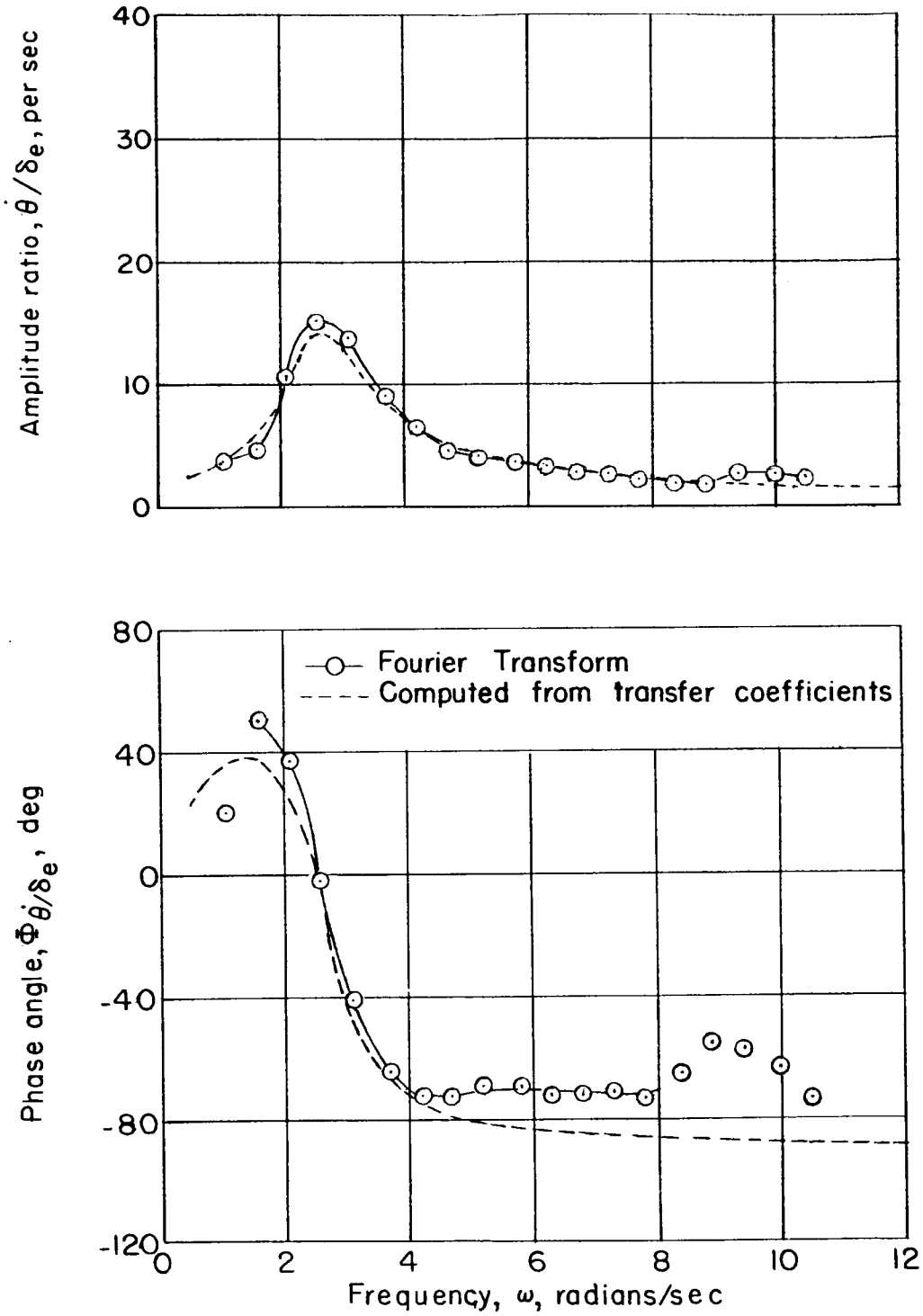

(h) M = 0.590; h_p = 31,000 feet.

Figure 9.- Continued.

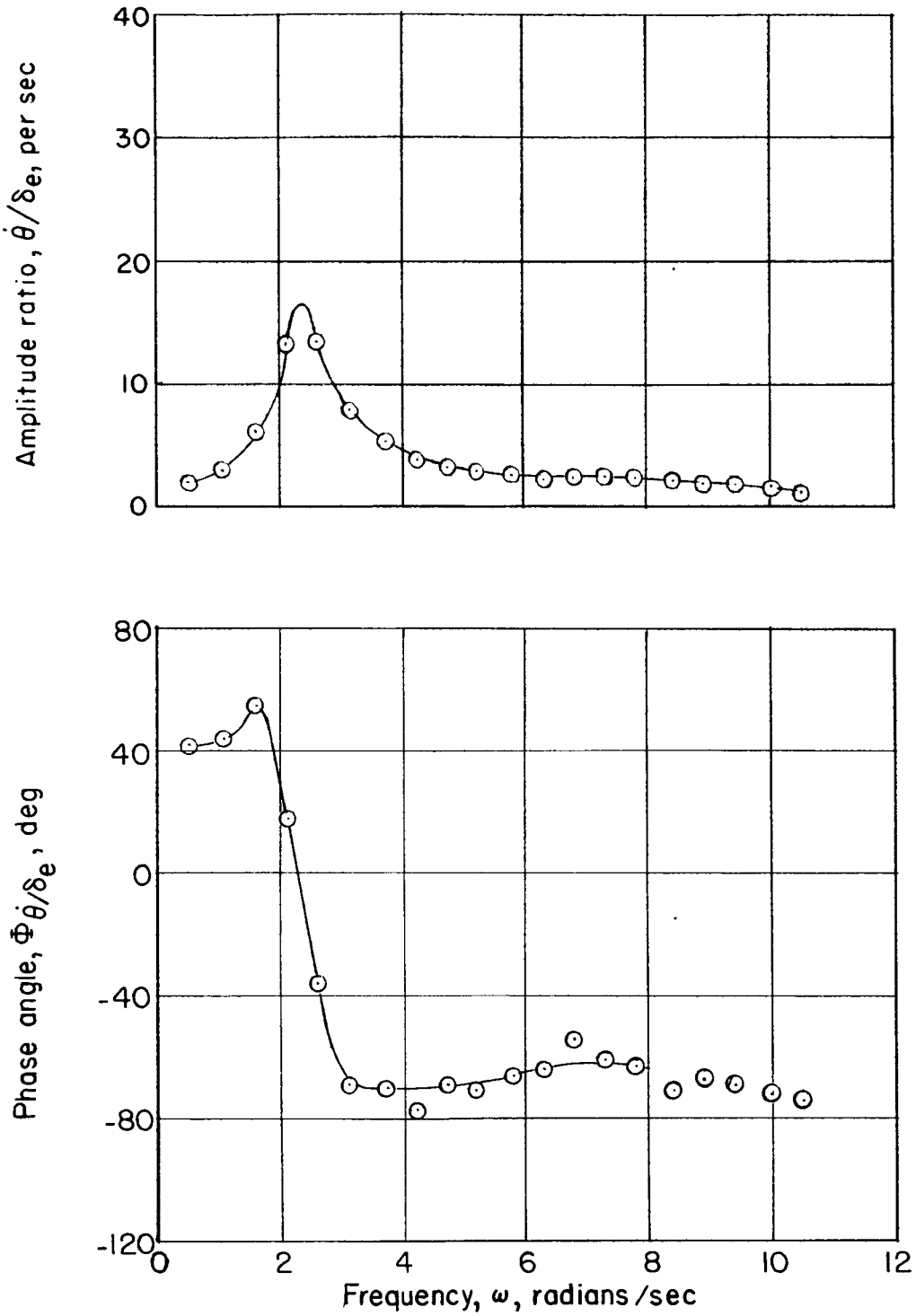

(i) M = 0.540; h_p = 30,000 feet.

Figure 9.- Continued.

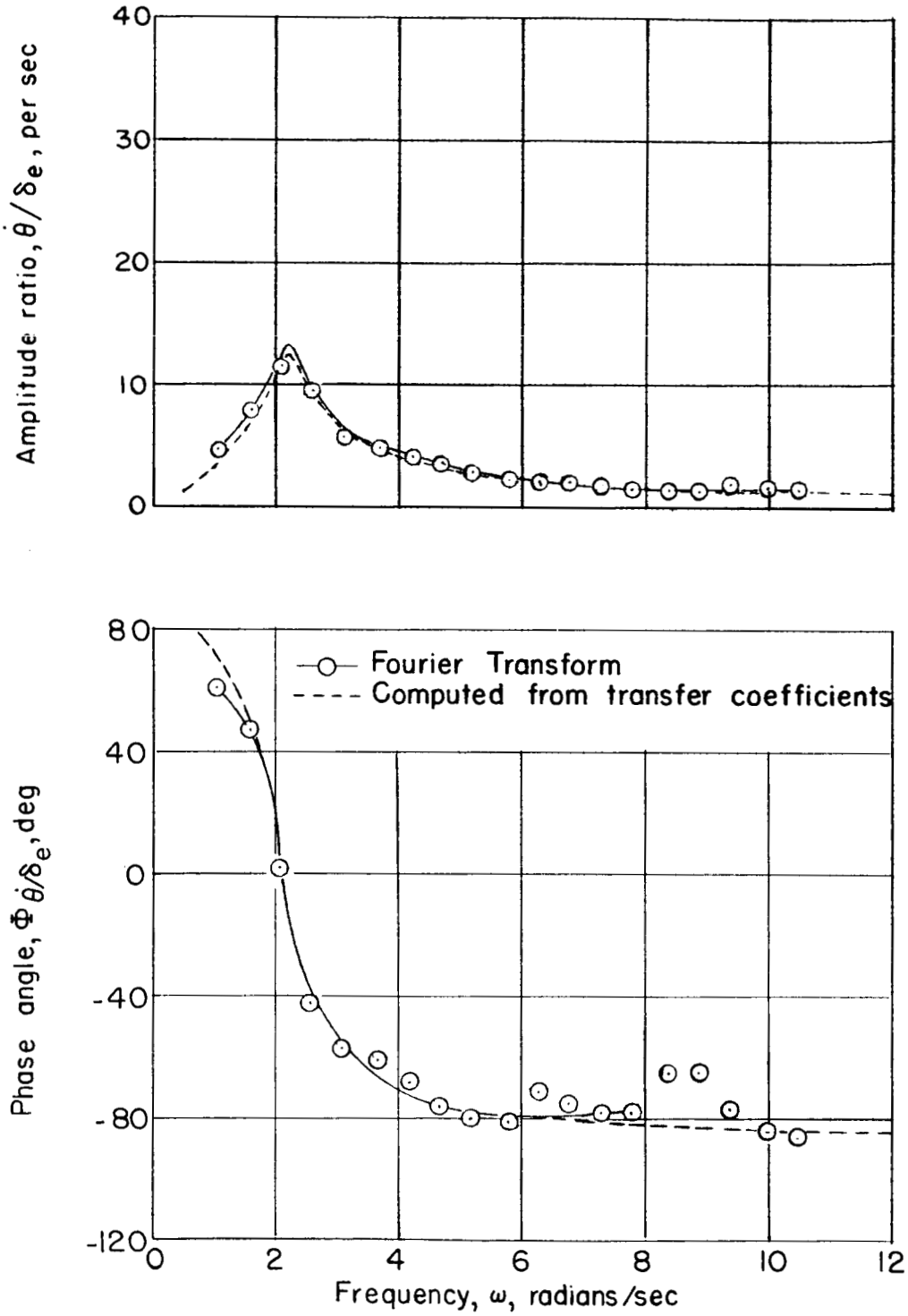

(j) M = 0.490; h_p = 30,000 feet.

Figure 9.- Concluded.

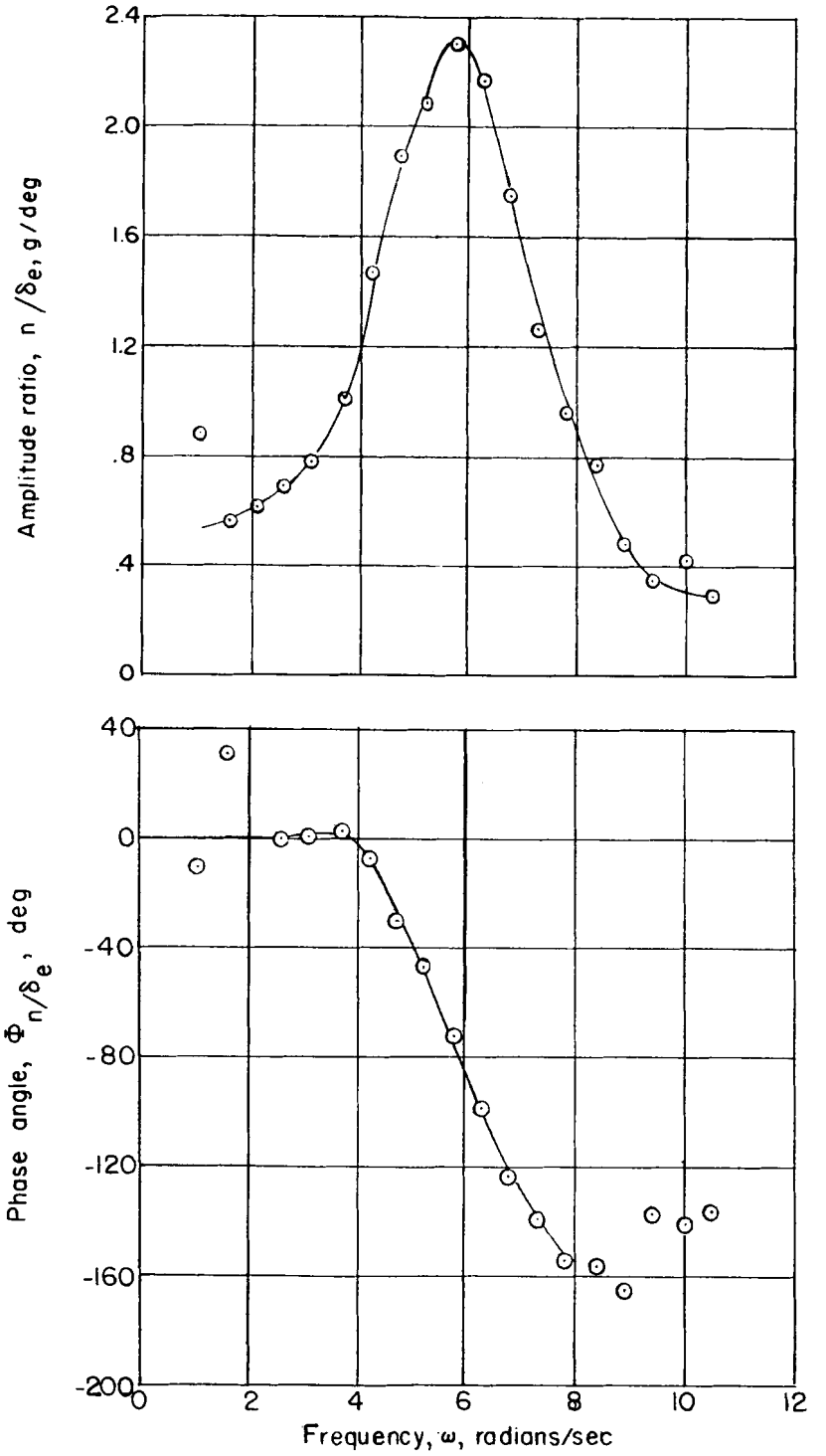

(a) M = 0.945; h_p = 32,000 feet.

Figure 10.- Normal acceleration frequency response characteristics for various Mach numbers.

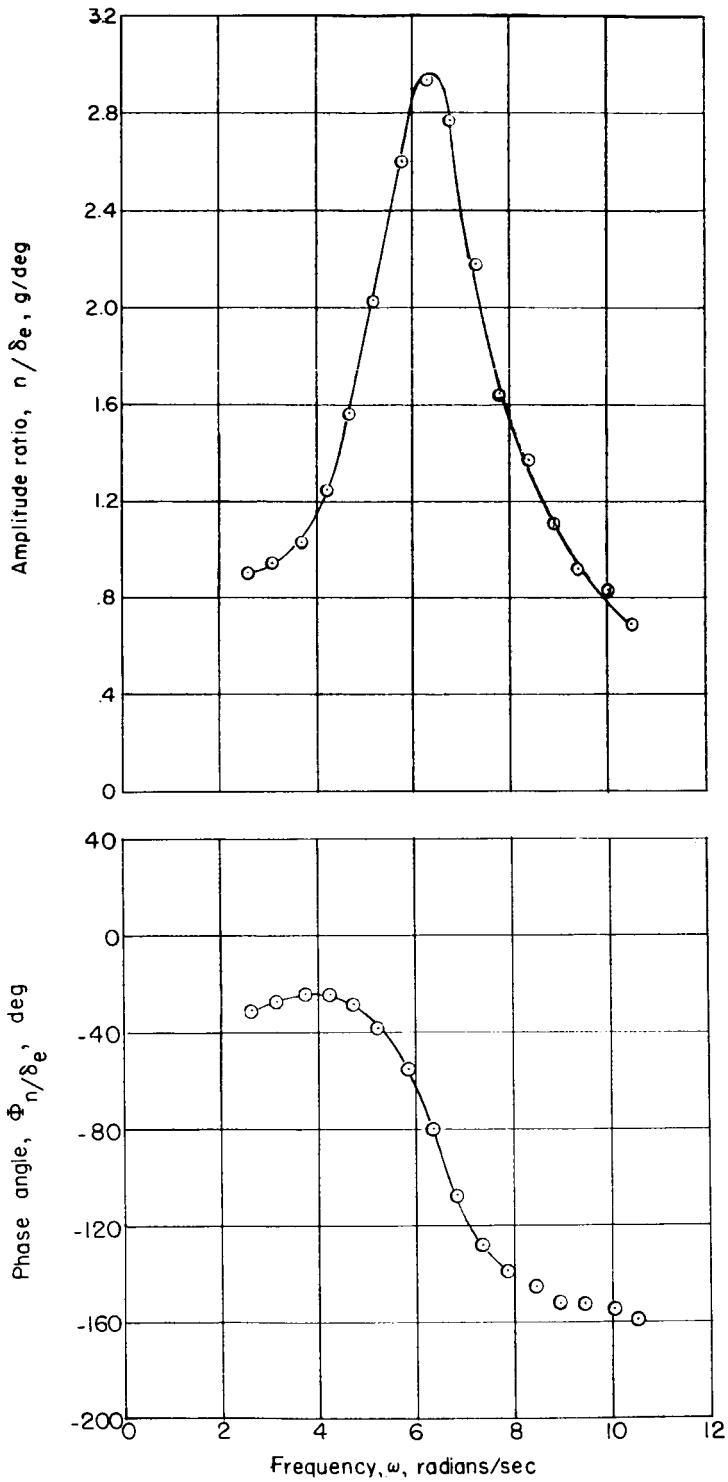

(b) M = 0.910; h_p = 27,000 feet.

Figure 10.- Continued.

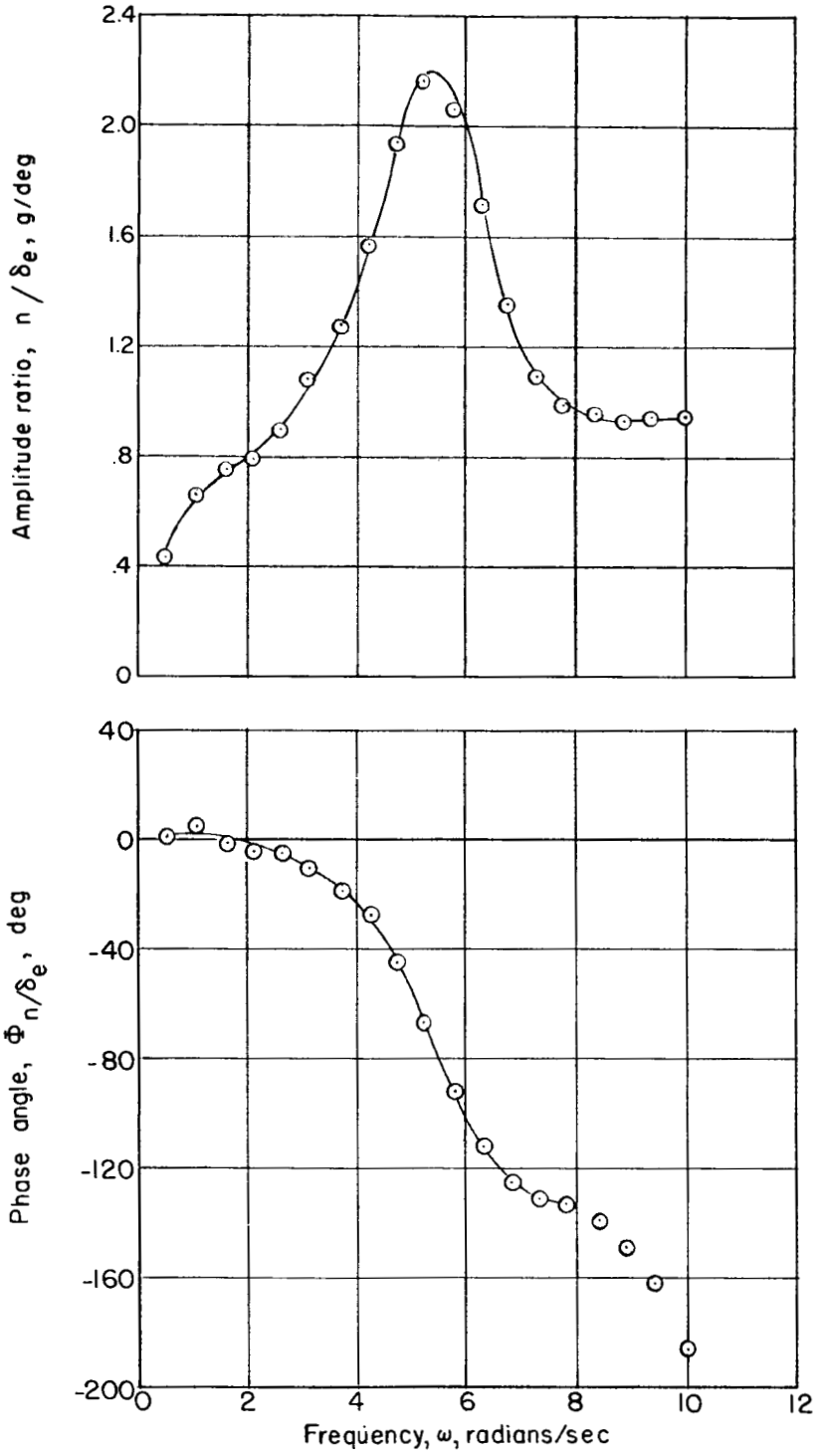

(c) M = 0.890; h_p = 30,000 feet.

Figure 10.- Continued.

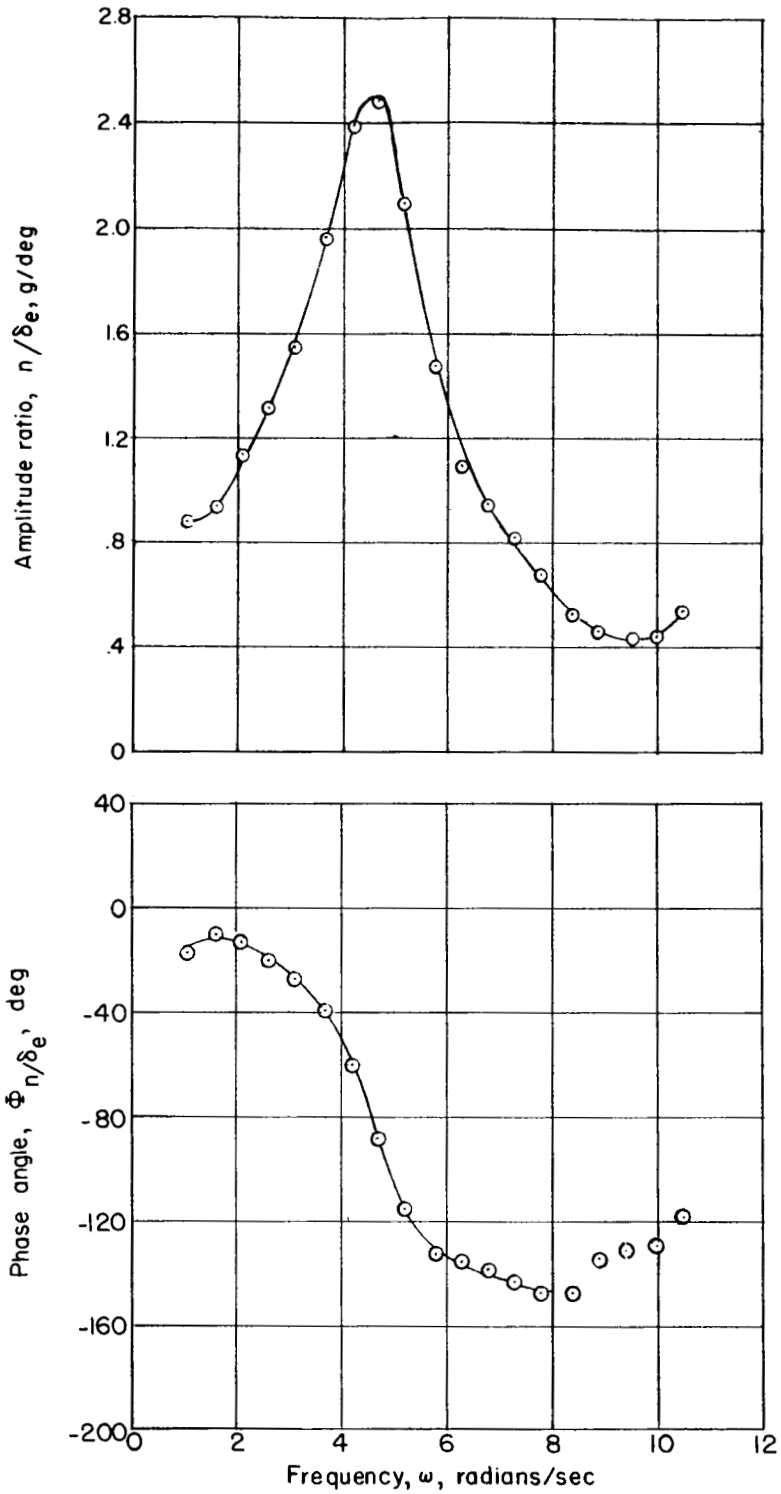

(d) M = 0.840; h_p = 28,000 feet.

Figure 10.- Continued.

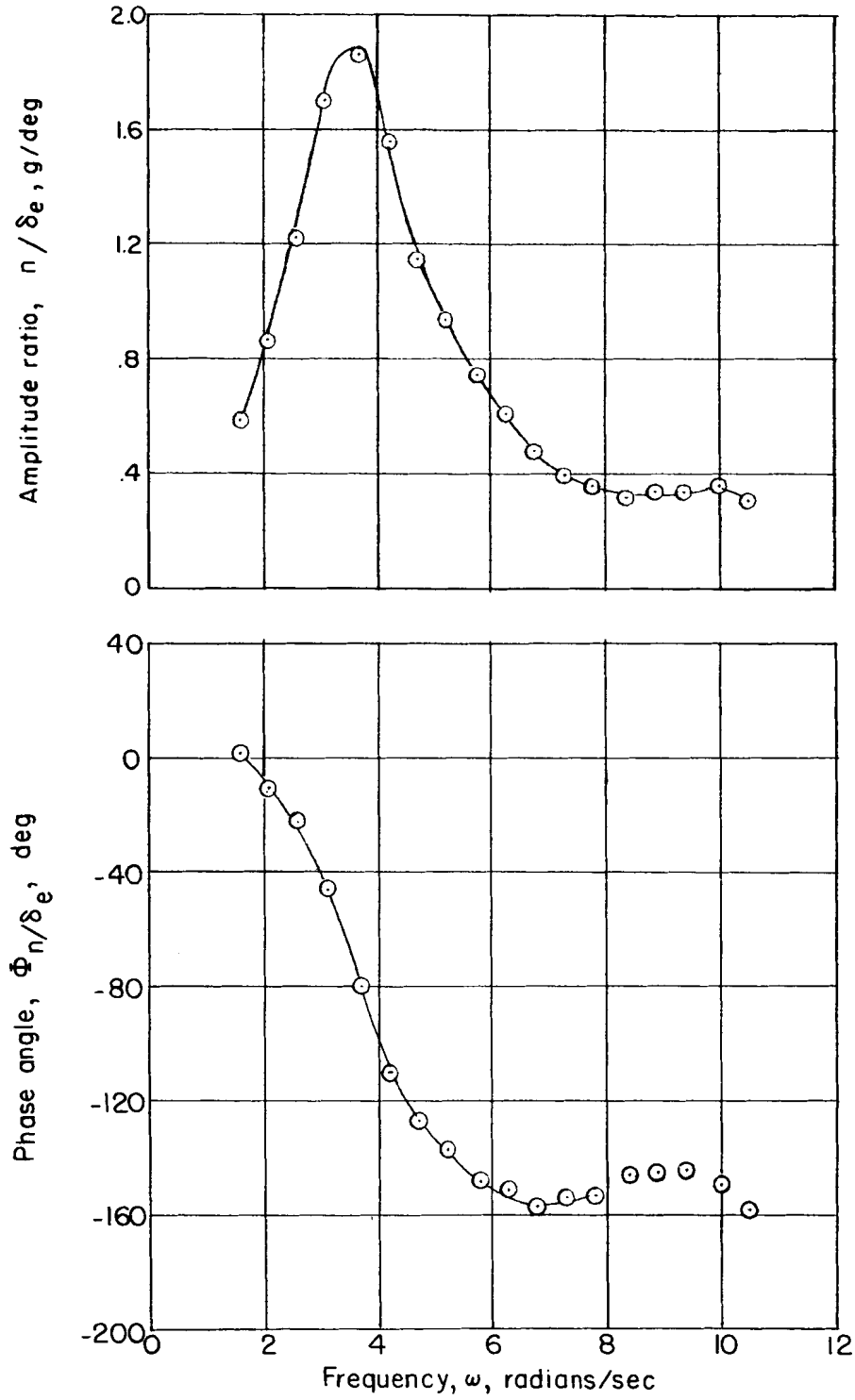

(e) M = 0.770; h_p = 31,000 feet.

Figure 10.- Continued.

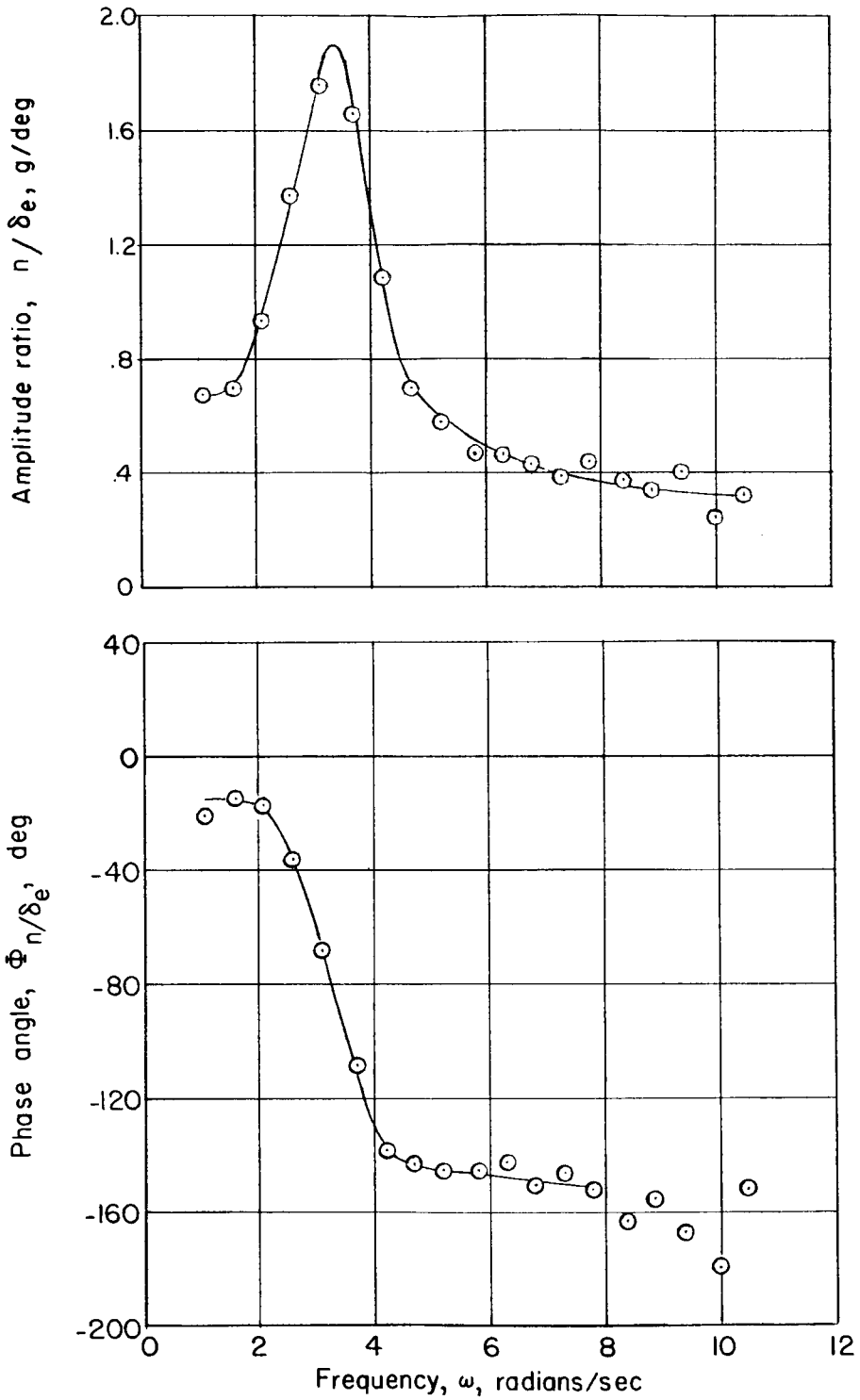

(f) M = 0.720; h_p = 31,000 feet.

Figure 10.- Continued.

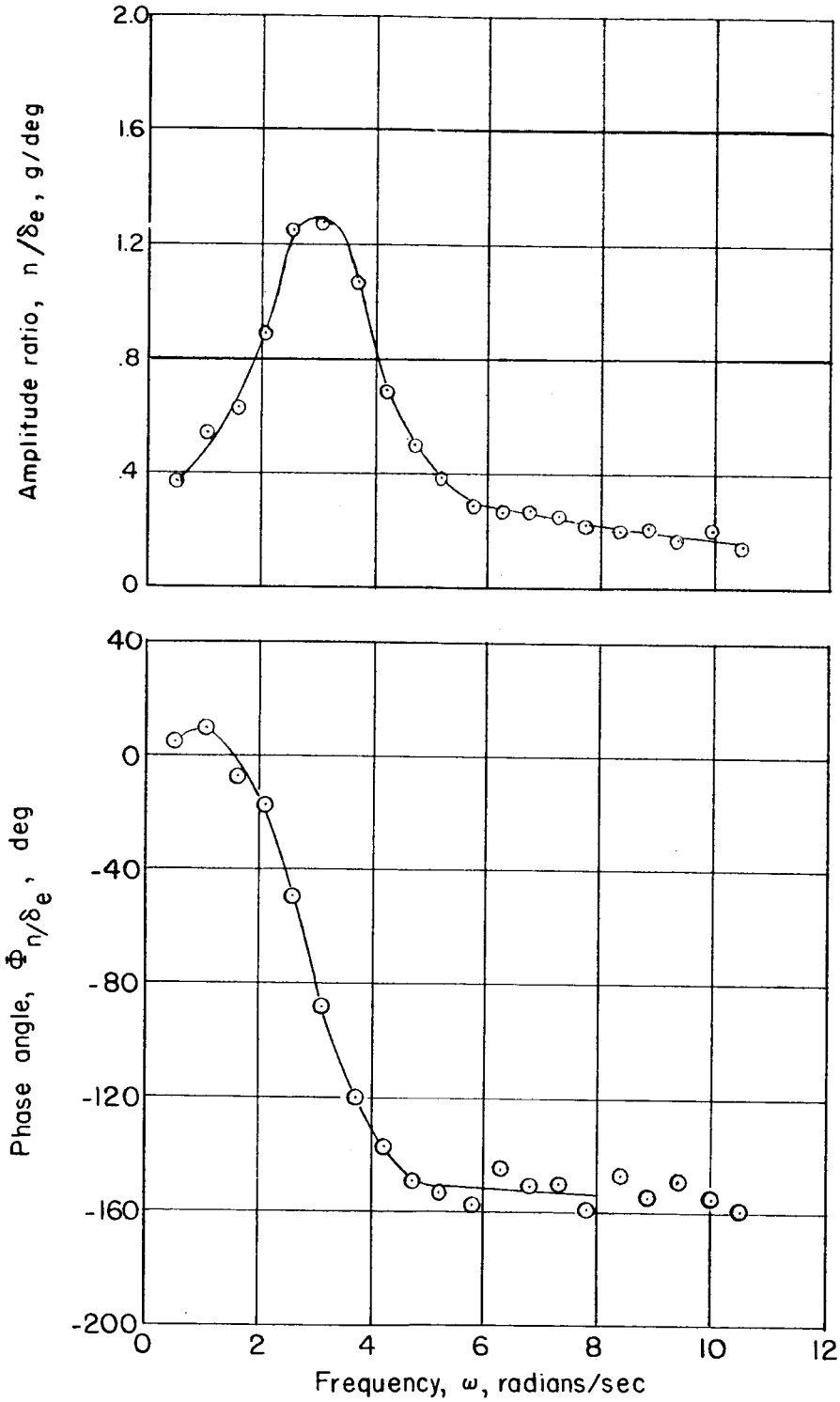

(g) M = 0.640; h_p = 30,000 feet.

Figure 10.- Continued.

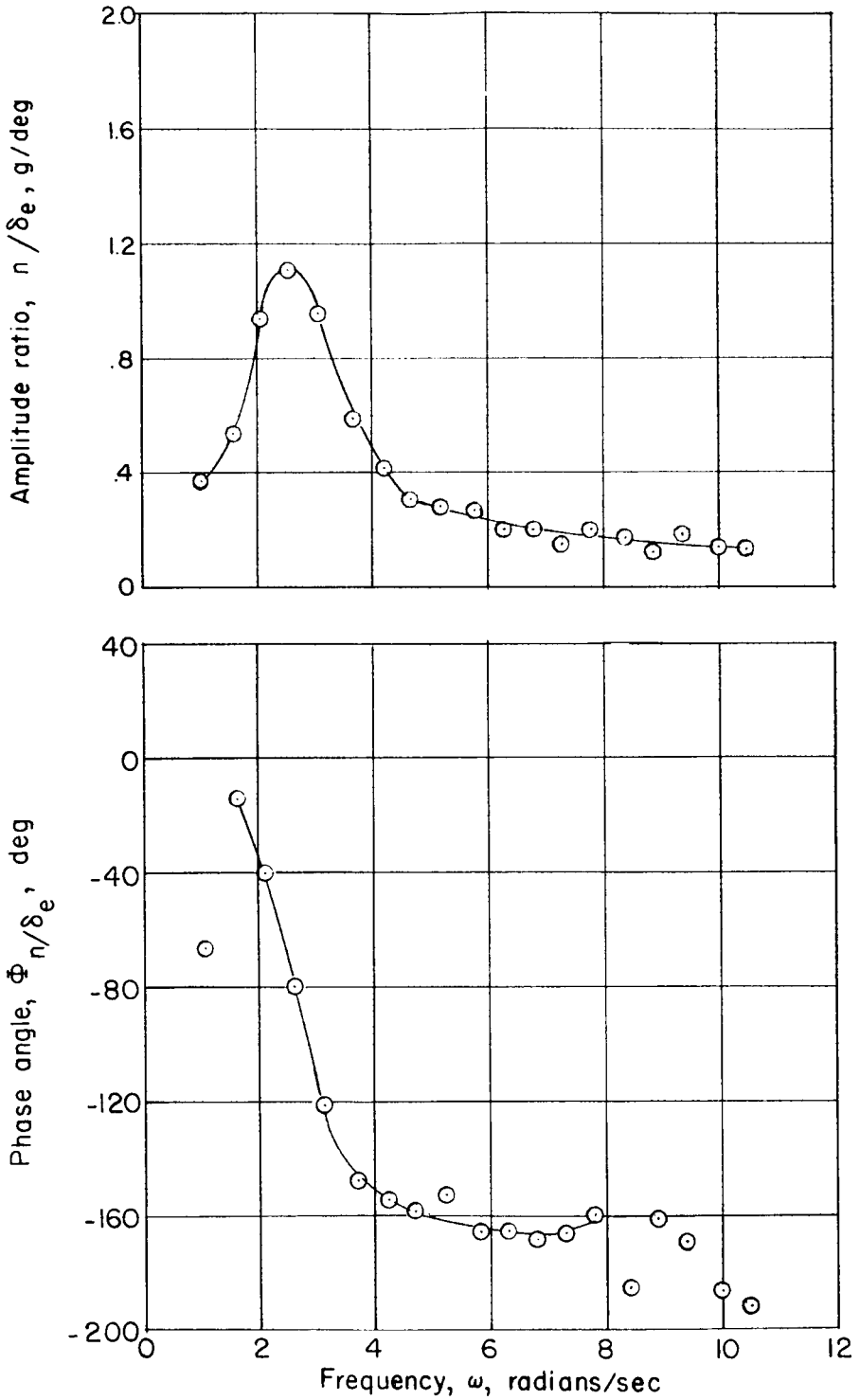

(h) M = 0.590; h_p = 31,000 feet.

Figure 10.- Continued.

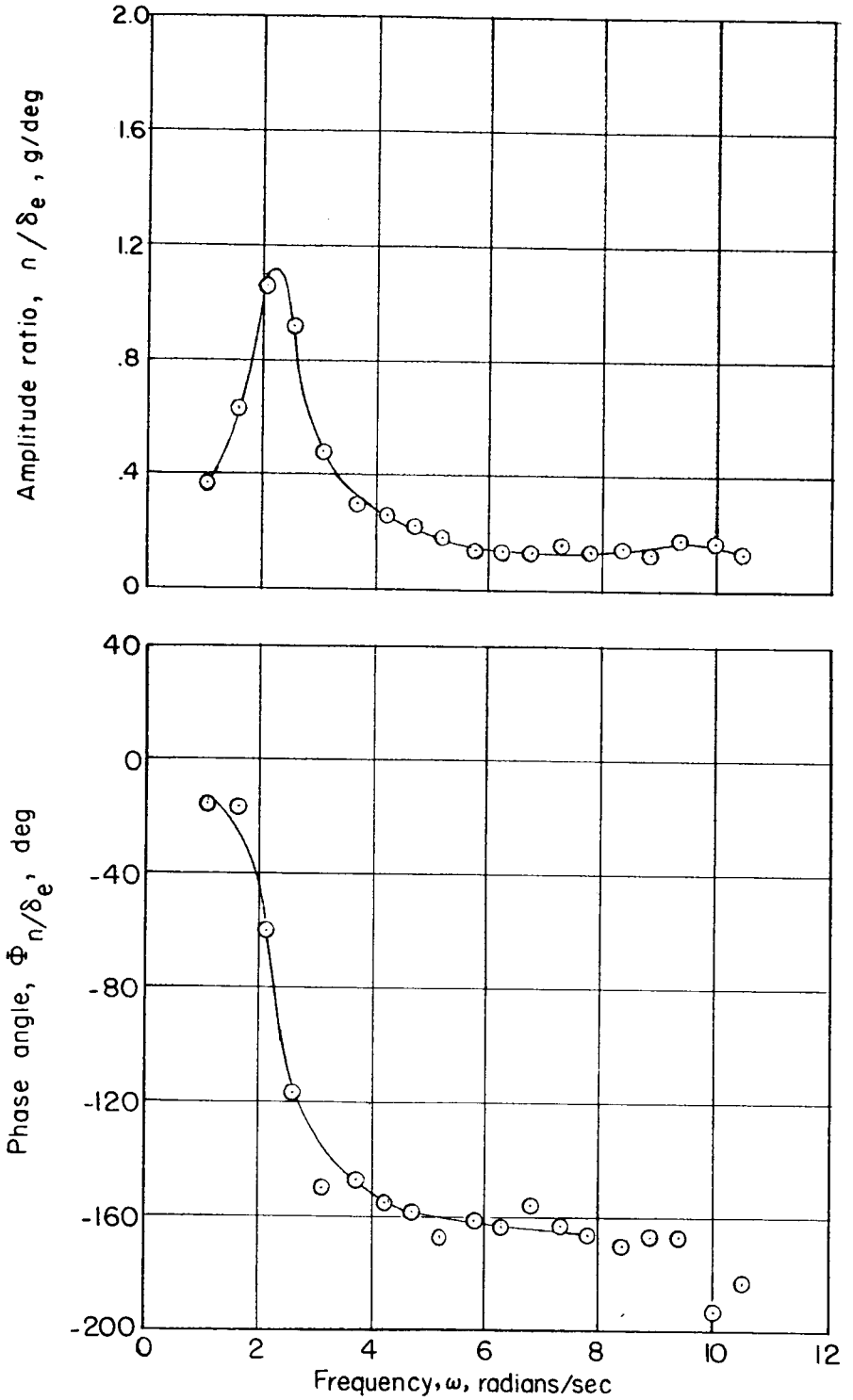

(i) M = 0.540; h_p = 30,000 feet.

Figure 10.- Continued.

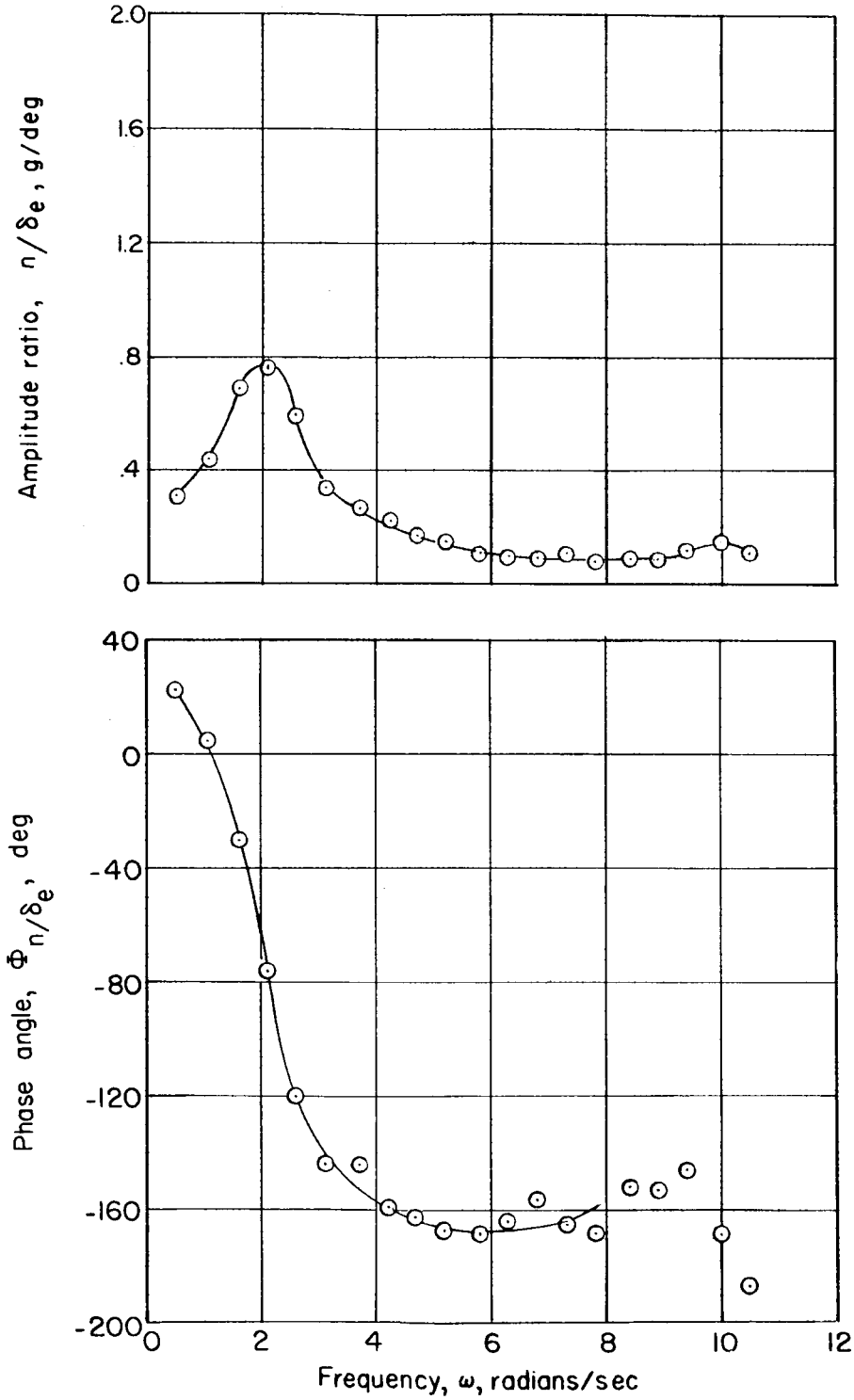

(j) M = 0.490; h_p = 30,000 feet.

Figure 10.- Concluded.

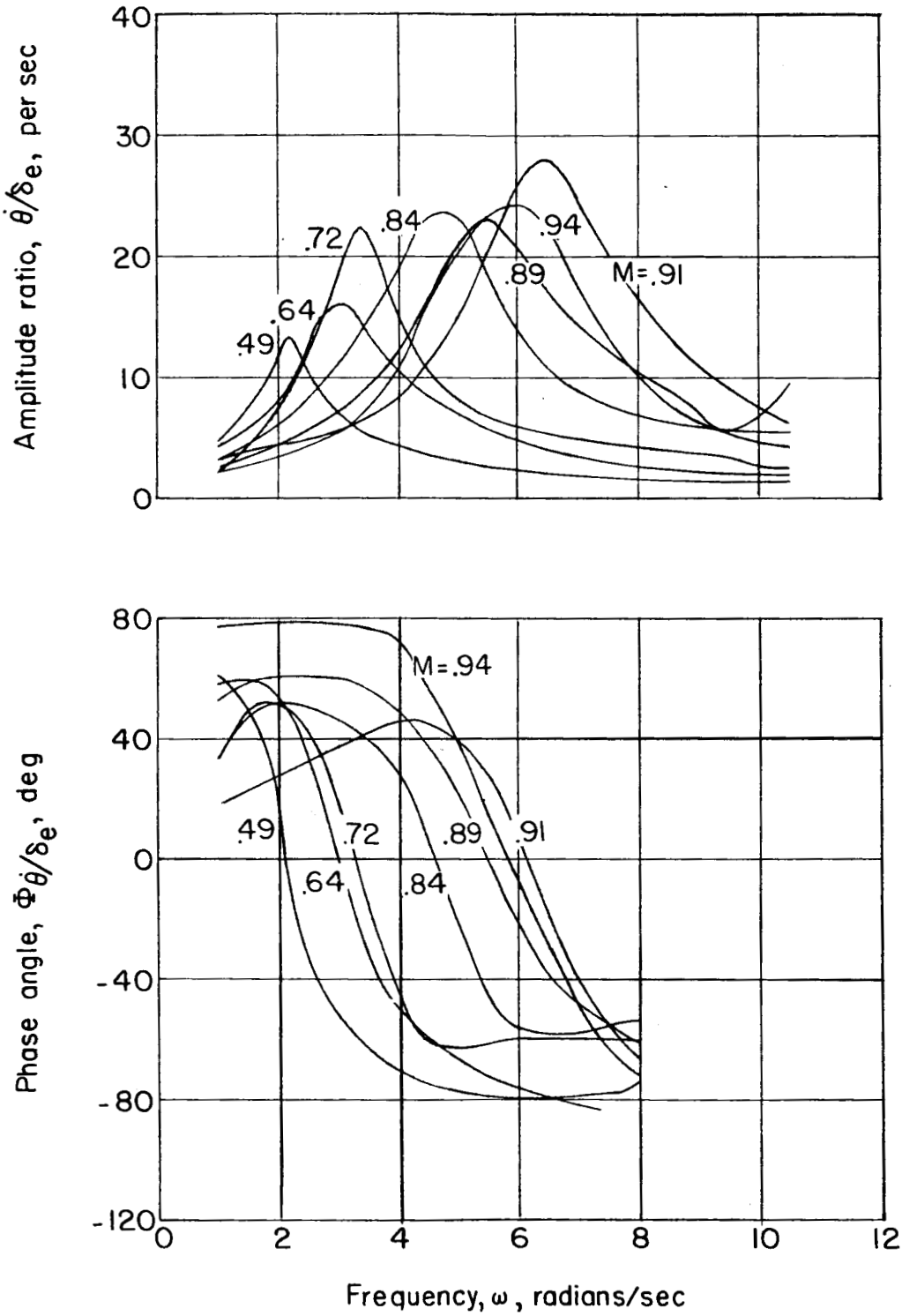

(a) Pitching velocity frequency response.

Figure 11.- Summary of the airplane frequency response characteristics.

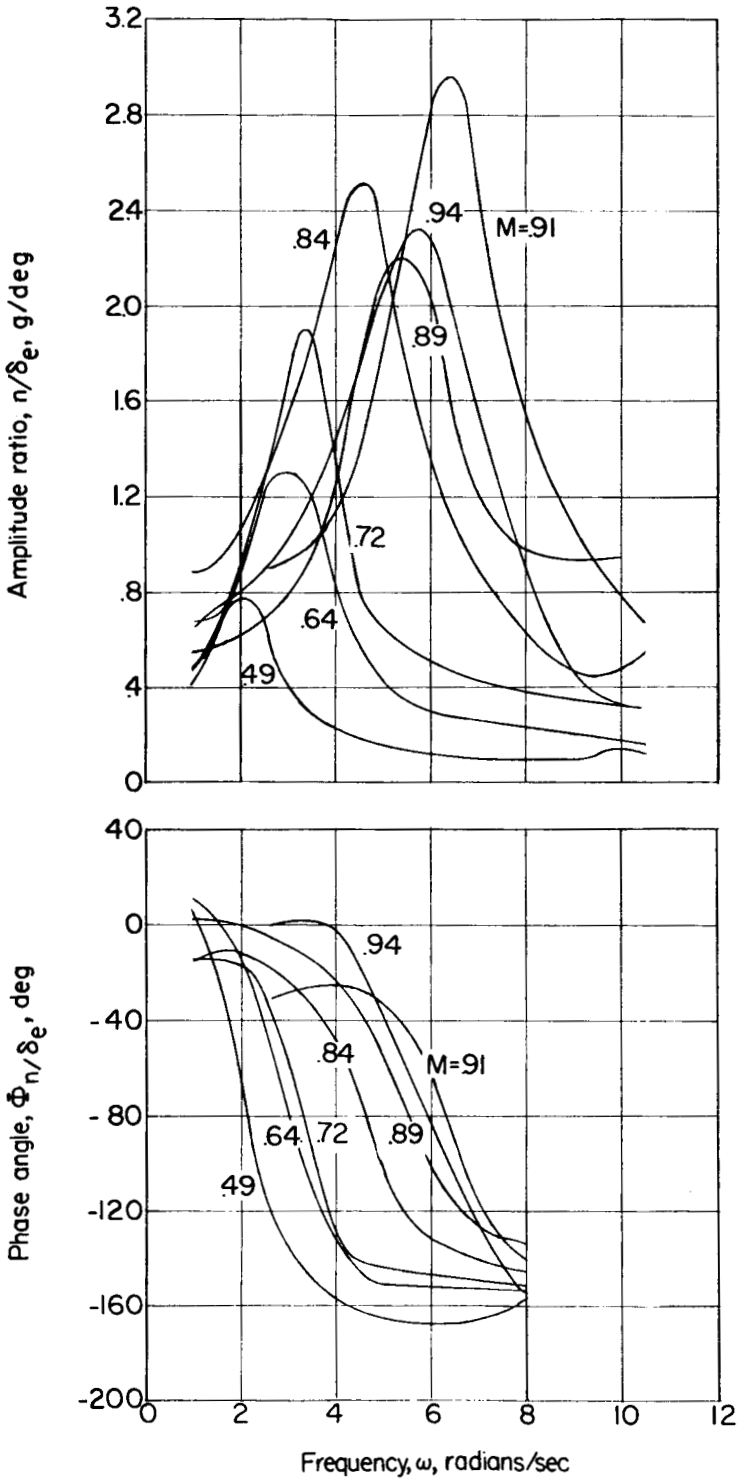

(b) Normal acceleration frequency response.

Figure 11.- Concluded.